2-16-2005

The Chromospheric Activity and Ages of M Dwarf Stars in Wide Binary Systems

Nicole M. Silvesteri
Department of Astronomy, University of Washington, nms@astro.washington.edu

T. D. Oswalt
Florida Institute of Technology, oswaltt1@erau.edu

Suzanne L. Hawley
Department of Astronomy, University of Washington, slh@astro.washington.edu

Accepted for publication in the Astronomical Journal, May 2005
Preprint typeset using LaTeX style emulateapj v. 6/22/04

THE CHROMOSPHERIC ACTIVITY AND AGES OF M DWARF STARS IN WIDE BINARY SYSTEMS[1]

Nicole M. Silvestri[2], Suzanne L. Hawley[2], and Terry D. Oswalt[3]

Accepted for publication in the Astronomical Journal, May 2005

ABSTRACT

We investigate the relationship between age and chromospheric activity for 139 M dwarf stars in wide binary systems with white dwarf companions. The age of each system is determined from the cooling age of its white dwarf component. The current limit for activity-age relations found for M dwarfs in open clusters is 4 Gyr. Our unique approach to finding ages for M stars allows for the exploration of this relationship at ages older than 4 Gyr. The general trend of stars remaining active for a longer time at later spectral type is confirmed. However, our larger sample and greater age range reveals additional complexity in assigning age based on activity alone. We find that M dwarfs in wide binaries older than 4 Gyr depart from the log-linear relation for clusters and are found to have activity at magnitudes, colors and masses which are brighter, bluer and more massive than predicted by the cluster relation. In addition to our activity-age results, we present the measured radial velocities and complete space motions for 161 white dwarf stars in wide binaries.

Subject headings: stars: activity — stars: ages — stars: binaries — stars: low-mass — stars: white dwarfs — techniques: spectroscopic

1. INTRODUCTION

The study of stellar activity has long been restricted to observed features on the surface of the Sun and to bright solar-type stars (Byrne 1993; Byrne & Doyle 1990). Studies conducted by, among others, Wilson (1966), Skumanich (1972), and Noyes et al. (1984) showed a link between activity in solar-type stars and the stellar rotation rate. An $\alpha\Omega$ dynamo driven by differential rotation at the radiative-convective boundary layer is thought to be the primary driver behind stellar activity in F, G, K, and early M stars. It is also believed to be responsible for the heating of the stellar chromosphere and corona as well as the production of star spots, flares, and prominences.

Recently, the study of stellar activity has been extended to include the entire M dwarf sequence. At first glance the magnetic activity observed in these low mass stars appears similar to that found in solar type stars, and in some cases is particularly strong. The dynamo generation mechanism must be different however, as these stars should be fully convective and therefore lacking the radiative-convective boundary layer responsible for magnetic dynamo generation in more massive stars (cf. Pettersen & Hawley 1989; O'Neal, Neff, & Saar 1998; Ding & Fang 2001; Martín & Ardila 2001).

Due to their slow burning of core hydrogen, M dwarfs that formed at the birth of the Galaxy are still on the main sequence and therefore retain information from the Galaxy's earliest epochs of star formation. In this study we investigate the relationship between magnetic activity and age for M dwarfs, with the goal of developing an age-activity relation that can be used to determine ages for this important and ubiquitous population.

Stellar age is one of the most difficult properties of a star to determine. Skumanich (1972) showed that chromospheric activity and age are related for solar-type stars by:

$$F(\text{Ca K}) = At^{-1/2}, \tag{1}$$

where F(Ca K) is the equivalent width of the Ca II K chromospheric emission line (in Å), A is a constant, and t is the age of the star (in years). The common explanation for this effect is that as the star ages, its rotation slows due to mass and angular momentum loss. This leads to a weakening of the internal rotationally-driven dynamo, causing a decrease in magnetic heating and hence chromospheric activity. Calibration of the chromospheric activity−age relation for F, G, and K stars has been carried out by Barry (1988) and Soderblom, Duncan, & Johnson (1991). However, a similar relation does not appear to hold for the M dwarfs. Stauffer et al. (1991) originally showed that all stars redder (lower temperature, lower mass) than a given $R-I$ color had Hα emission in the Pleiades and Hyades clusters. The color at the "Hα limit" was bluer, corresponding to a higher mass where activity still occurred, in the younger cluster. This result led to the speculation that both mass and age affect the Hα limit. A subsequent study of six open clusters (IC2602, IC2391, NGC2516, Pleiades, Hyades, and M67 Hawley, Reid, & Tourtellot 2000, hereafter HRT) showed that there was a linear re-

[1] Based on observations obtained with the Apache Point Observatory (APO) 3.5-meter telescope, which is owned and operated by the Astrophysical Research Consortium (ARC); The Cerro Tololo Inter-American Observatory (CTIO) 4.0-meter telescope, which is operated by the Association of Universities for Research in Astronomy (AURA) Inc., under a cooperative agreement with the National Science Foundation (NSF) as part of the National Optical Astronomy Observatories (NOAO), which also operates Kitt Peak National Observatory in Tucson, Arizona; and the SARA Observatory 0.9-meter telescope at Kitt Peak, which is owned and operated by the Southeastern Association for Research in Astronomy (`http://www.saraobservatory.org`).

[2] Department of Astronomy, University of Washington, Box 351580, Seattle, WA 98195, nms@astro.washington.edu, slh@astro.washington.edu.

[3] Department of Physics & Space Sciences and the SARA Observatory, Florida Institute of Technology, 150 W. Univ. Blvd.,

the log(age) of the cluster. The $V-I$ color is directly related to the atmospheric temperature and therefore the mass of a main sequence M dwarf. The relationship was calibrated only for relatively young M dwarfs with ages < 4 Gyr (the age of M67, the oldest open cluster in their study). Thus, HRT confirmed that activity in M dwarfs is a function of age at a given mass (or alternatively mass at a given age), quite unlike the rotationally-dependent Skumanich relation for F−K stars, which appears to be independent of mass. The HRT age-activity relationship was used by Gizis, Reid, & Hawley (2002) to constrain the ages of brown dwarf stars in binaries with M dwarf companions and to study the star formation history of the Galactic disk.

Unfortunately, it is not yet feasible to spectroscopically determine the activity levels of older M dwarfs in either open or globular clusters, because the clusters are faint and distant, making the observations difficult even on the largest telescopes. Therefore, the current activity−age relation determined with the use of clusters only allows for the sampling of stars formed well after the earliest epochs of star formation in the Galaxy. Further progress in pinning down the old, low mass end of the M dwarf chromospheric activity−age relation must therefore come from another method.

Here we describe our analysis of a sample of $\sim$ 200 spectroscopically identified M dwarf stars in common proper motion binary (CPMB) systems with white dwarf (WD) companions. The age of the system is determined from the cooling age of the companion WD, assuming the WD and M dwarf are coeval. The WD ages are accurate to roughly 25% (or better if the mass of the WD is known), comparable to the accuracy determined from the ages of clusters. Since many binaries in our sample have ages well beyond the present 4 Gyr cluster limit, this allows us to examine the activity−age relation for much older M dwarfs. Concurrently, our sample provides a significant amount of new data on WD stars in binary systems.

Using the spectra of the M dwarfs, we determine the spectral types (masses) and from the photometry of the WDs we determine the age of each pair in which activity is observed. In addition, we determine the radial velocities of the M stars and, since proper motions are known, the complete space motions for all systems in the observed sample. This allows us to examine the kinematics and provides an independent indicator of population membership.

The paper is organized as follows: In §2 we introduce the sample and selection criteria, and describe the observations, data reduction and determination of M dwarf atmospheric parameters. Our method for estimating ages of the WDs using atmospheric and evolutionary models is presented in §3. In §4 we examine the spectroscopic and photometric properties of the active M dwarfs and present the final activity−age results for the sample. We discuss the kinematics of the sample and the implications of these results in §5, building on the earlier work in Silvestri, Oswalt, & Hawley (2002). Our conclusions are summarized in §6.

2. SAMPLE SELECTION AND OBSERVATIONS

Luyten (1963, 1969, 1974, 1979) and Giclas, Burnham, & Thomas (1971, 1978) first identified several proper motion-selected surveys from the original Palomar Observatory Sky Survey (POSS) plates and the photographic plates from Lowell Observatory. The Luyten−Giclas CPMB systems have relatively wide orbital separations ($\langle a \rangle \sim 10^3$ A.U., Oswalt et al. 1993). Unlike close binary systems, these wide pairs are not influenced by mass exchange and evolve essentially as two single stars. The stars that make up a CPMB (or multiple component) system originally evolved from the same molecular cloud (Boss 1987, 1988; Pringle 1989) and are therefore taken to be coeval. Of particular interest to our study are those CPMBs which contain one WD and one main sequence M dwarf star (we will refer to these systems as WD+dM pairs). Among these pairs are some with very faint and cool (hence old) WD stars (Liebert, Dahn, & Monet 1988; Oswalt et al. 1996), which are particularly useful for setting a firm lower limit to the age of the Galaxy. Here we also show that they are useful for extending the age range of the age-activity relationship.

A subset of 196 systems was selected for observation (see Table 1). The sole selection criterion was that the system must contain spectroscopically identified WD and M dwarf stars. Low resolution spectra (7−15 Å pixel^{-1}, Oswalt, Hintzen, & Luyten 1988; Oswalt et al. 1991, 1993) were used to confirm the rough spectral type of each CPMB component. Of the 196 systems, 189 are binary (WD+dM) and seven are triple systems (one WD+dM+dK, one WD+dM+dG, three WD+dM+dM, and two WD+WD+dM). This gives a total of 199 M dwarf stars with at least one WD companion. Table 1 lists all 196 system names as assigned by Luyten in column 1, their R.A. and Decl. (coordinates are for equinox 1950; columns 2 & 3), the V magnitude and original low resolution spectroscopic identification (columns 4-7), the site, date, and exposure time at which the object was observed (columns 8-10). Columns 11-14 list the proper motion, direction of proper motion (measured east of north), position angle (centered on the primary measured east of north), and the separation of the components, respectively.

The biases in our sample, imposed primarily by the sampling area, proper motion (μ) criteria, and limiting apparent magnitude (in this case photographic magnitude, $m_{\rm pg}$) of the original surveys, are well understood (see Oswalt & Smith 1995; Smith & Oswalt 1995; Oswalt et al. 1996; Wood & Oswalt 1998). Our sample includes objects north of declination $-60°$ excluding the most dense regions of the Galactic plane ($|b| < 15°$). It thus includes $\sim$ 65% of the visible sky (Dawson 1986). The Luyten−Giclas binaries are restricted to $0.1 \leq \mu \leq 2''.5$ yr^{-1} (La Bonte 1970), a limit based solely on Luyten's ability to discern motion between the original and retake plates of the POSS. The magnitudes of the CPMBs are $m_{\rm pg} \leq 20$, i.e. down to the rough magnitude limit of the POSS blue plate. It should also be noted that because Luyten avoided listing pairs that he knew had already been discovered by Giclas, the latter need to be included in any sample where completeness is important.

2.1. *Spectroscopic Observations*

The northern portion of the sample was observed spectroscopically during 32 half-nights on the ARC 3.5-m telescope at APO. Observations were performed on the

(∼ 2 Å/pixel) with a 1″.5 slit. With this setup, slits were centered at 6700 Å (red) and 4600 Å (blue) yielding wavelength coverage of ∼6000-7500 Å and ∼4000-5200 Å, respectively. An additional three full nights of observing time on the CTIO 4-m Blanco telescope were used to observe the systems which could not be seen from the northern hemisphere. Observations were performed with the R−C Spectrograph in medium-resolution mode (∼ 4 Å/pixel) and a 1″.0 slit. The grating tilt was centered at 6800 Å and covered a wavelength range of ∼3500-8500 Å. A condensed Journal of Observations is given in Table 2 where the first three columns give the UT date of the observing run followed by the site (column 4), the average seeing for the night (column 5), and some notes on the weather conditions (column 6).

We were unable to observe ten (40Eri−C, LP36−142, LP369−14, LP321−397, LP321−459, LP458−48, CD-51°13128, L427−61, LP411−22, and L573−109) of the 196 systems in our original sample (see Table 1). 40Eri−C was too close to its extremely bright companion to be observed. LP36−142, LP369−14, LP321−397, and LP321−459 were all too faint ($m_{\rm pg} \geq 19.5$) to be observed in reasonable exposure times. The proper motion of the system LP458−49/48 has moved the M star (LP458−48) into the glare of a bright field star. CD−51°13128, L427−61, LP411−22, and L573−109 were not observed due to weather on the evenings on which they were slated for observation.

The data were reduced with standard *IRAF*[5] reduction procedures. In all cases, program objects were reduced with calibration data (bias, flat, arc, flux standard) taken on the same night. Data were bias subtracted and flat-fielded, and one-dimensional spectra were extracted using the standard aperture extraction method. A wavelength scale was determined for each target spectrum (including the flux and M dwarf standards) using He-Ne-Ar arc lamp calibrations. Flux standard stars were used to place the spectra on a calibrated flux scale. We emphasize that the final flux calibrations for the targets are only relative fluxes as most nights were not spectrophotometric.

After final reductions and close inspection of the individual spectra, we eliminated 28 M dwarfs from the final analysis because of insufficient signal to noise in the spectra. An additional 22 binaries were eliminated due to problems with the WD photometry as outlined in Smith (1997). This left 139 WD+dM binaries for final analysis in the activity−age relation in §4 and 161 M dwarf stars for the kinematics discussion in §5 (kinematics of the system are based on the M star so the 22 systems with poor WD photometry are included in this portion of the study).

2.2. *Spectroscopic Measurements*

The spectral types of the M dwarfs were determined by measuring the strength of Titanium Oxide (TiO) molecular features in the spectra, using flux ratios at strong bandheads as described in Reid, Hawley, & Gizis (1995). We used observations of M dwarf standards obtained at APO to calibrate the spectral type scale for our program as described in Kirkpatrick, Henry, & McCarthy (1991) and Hawley et al. (2002), and found that our results agreed well with Reid, Hawley, & Gizis (1995). The uncertainty in M dwarf spectral type for this procedure is ± 0.5 spectral type at the APO resolution and ± 1.0 spectral type at the CTIO resolution. Figure 1 plots our measured TiO5 bandstrengths against the catalog spectral type. As displayed in the Figure the equation for the line of best fit is

$$\mathrm{Sp} = -11.17 \times \mathrm{TiO5} + 8.21, \sigma_{\rm rms} = \pm 0.52. \quad (2)$$

The relation adopted for this (TiO5, Sp) calibration by Reid, Hawley, & Gizis (1995) for their sample of 88 M dwarf standards defined by Kirkpatrick, Henry, & McCarthy (1991) is

$$\mathrm{Sp} = -10.775 \times \mathrm{TiO5} + 8.2, \sigma_{\rm rms} = \pm 0.5. \quad (3)$$

Clearly, the relation is in good agreement with the larger sample of standards from Reid, Hawley, & Gizis (1995).

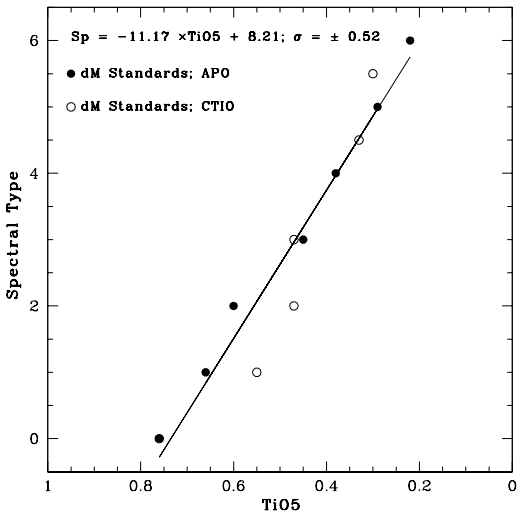

FIG. 1.— The measured TiO5 bandhead strength versus catalog spectral type (Reid, Hawley, & Gizis 1995). The straight line denoted by the equation on the plot is the adopted relation for our sample over the range dM0 ≤ Sp ≤ dM6. The filled circles are standards observed at APO with ∼ 2 Å/pixel resolution and uncertainty of ± 0.5 spectral type. The open circles are from the lower resolution spectra observed at CTIO with ∼ 4 Å/pixel resolution and indicate an uncertainty of ± 1.0 spectral type.

Calcium Hydride (CaH) features were also measured, as the relative strength of CaH compared to TiO serves to identify subdwarfs as described in Reid & Gizis (1998). We found only one possible subdwarf in the sample, LP164-52.

The equivalent width (EW) of the Hα emission line, which is formed in the magnetically heated chromosphere and is commonly used to characterize the magnetic activity of M dwarfs, was measured following the prescription in Hawley, Gizis, & Reid (1996). The Hα EW may change dramatically through the M dwarf sequence solely because of the rapidly changing continuum flux in this wavelength region, and not because of a change in the magnetic heating of the chromosphere. However, all of our analysis is carried out on subsamples of objects with the same spectral type, so comparing relative equivalent widths within these subsamples gives a reasonable measure of differences in magnetic activity.

Table 3 gives the measured Hα EW and uncertainties

[5] *IRAF* is written and supported by the *IRAF* programming group at the NOAO in Tucson, Arizona. NOAO is operated by the AURA, under cooperative agreement with the NSF

hydride and TiO flux ratios are listed in columns 7-14 followed by the new spectral types as determined from the TiO5 bandheads (column 15). A reference column (16) indicates the designations (dMe, dM(e), or dM) for each M dwarf as discussed further in §4.1. The Hα EW and TiO5 ratios are displayed in Figure 2.

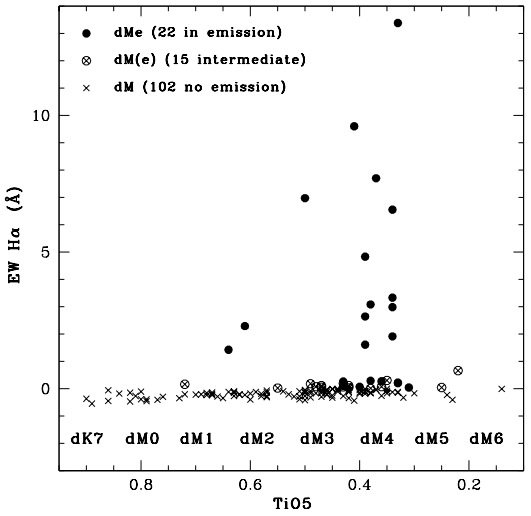

FIG. 2.— The EW in Å of the Hα feature for 139 dMs in CPMBs versus the ratio of the flux in the TiO5 molecular band. Filled circles are dMe stars. Open circles with crosses are dM(e) stars and crosses are inactive dM stars.

3. DETERMINATION OF WHITE DWARF AGES

We use the photometry of the WDs provided by Smith (1997) for our age determinations. This method introduces somewhat larger uncertainties in age than matching model H line profiles to high S/N data (e.g. Silvestri et al. 2001) but it is accurate enough for our purposes (see Oswalt et al. 1996; Smith 1997, for a discussion of this procedure). The cooling ages were extracted from the model grids as described in Bergeron, Saumon, & Wesemael (1995) using the $V-I$ and $B-V$ colors of the WDs.

The mass of the WD plays the dominant role in determining the WD cooling rate. Hence, it is not surprising that a large uncertainty in the final age from the WD models is associated with the mass estimate. Unfortunately, determining the mass of a WD is not a simple task, and achieving a high precision is even more daunting. At present, there are less than 300 individual WDs for which a mass has been determined and of those, less than 100 have been determined within $\sim 10\%$ precision ($\sigma < 0.05\ M_{\odot}$).

Silvestri et al. (2001) determined the masses for 44 WDs in the Luyten sample based on the gravitational redshift of the WD. These masses on average have $\sigma_{M_{\rm WD}} > 0.05\ M_{\odot}$. Silvestri et al. (2001) sampled a significant fraction of the WDs in our current sample. We use their mean mass of $0.61 \pm 0.16\ M_{\odot}$ as a representative mass of the WDs in our sample. Only three of the WDs in this study have independently measured masses and active (dMe) M dwarf companions (L170-14B, LP617-35, and LP798-13) and when these masses are used in the determination of the ages for these three systems, the ages determined from the mean mass. For consistency, we use the mean mass estimate for all of the WDs in this study. It appears to be a reasonable mean mass assumption since it is close to the mean mass of nearly every WD mass distribution in the literature (see for example Koester 1987; Bergeron, Saumon, & Wesemael 1995; Reid 1996).

Having established an average mass and uncertainty for the WDs in our sample, we next determined the gravities corresponding to our mean mass and error using the mass−radius relation implicit in the WD model calculations. For either the hydrogen- or helium-dominated model atmospheres, the average difference in cooling ages are less than 0.5 Gyr, approximately half the size of the errors imposed by assuming a mean mass for the WD. Adding errors from the photometry and from the mass estimate in quadrature yields the uncertainty in the cooling ages of the WDs for the pure H and He (DA and DB WDs, respectively) atmospheric model results. The average cooling age for our sample is $t_{\rm cool} = 3.06^{+0.94}_{-1.09}$ Gyr for a 0.61 $M_{\odot}$ mass WD.

3.1. *Initial→Final Mass Relation for White Dwarfs*

The ages and uncertainties calculated above represent the total cooling age of each individual WD (total time after emerging from the planetary nebula). This however, is not the total age of the WD. We need a way of estimating the length of time a 0.61 $M_{\odot}$ WD exists on the main sequence before evolving to become a WD. The pre-WD lifetime is dependent on the initial mass of the progenitor star. Therefore, it is necessary to determine the main sequence mass of the progenitor star based on the final WD mass. This process is complicated because the progenitor may lose a significant amount of mass during its evolution.

Weidemann (2000) discusses the many factors which determine the final mass of the WD such as rotation, binarity, magnetic fields, mergers, and differential mass loss. The average main sequence mass for a 0.61 $M_{\odot}$ WD from Weidemann (2000) is $2.17 \pm 0.19\ M_{\odot}$. Using the third-order polynomial of Iben & Laughlin (1989)

$$\log t_{\rm evol} = 9.921 - 3.6648(\log M_{\rm I}) + 1.9697(\log M_{\rm I})^2 - 0.9369(\log M_{\rm I})^3 \quad (4)$$

we determine the main sequence lifetime corresponding to a given initial mass, where $t_{\rm evol}$ is the main sequence lifetime (in years) of the star and $M_{\rm I}$ is the progenitor mass of the WD (in $M_{\odot}$).

For our $M_{\rm WD} = 0.61\ M_{\odot}$ WD mass, this translates into a main sequence lifetime of $0.75^{+0.21}_{-0.15}$ Gyr. We added this value to the individual cooling ages of the WDs ($t_{\rm cool}$) as determined in the previous section. This yields an average age for the WDs in our sample of $3.81^{+0.98}_{-1.09}$ Gyr, near the age of the oldest cluster (M67) in the previous activity−age relations determined by HRT.

4. AGE-ACTIVITY RESULTS

4.1. *Hα Emission*

In §2.3 we discussed how the EW of the Hα emission feature in M dwarfs is used as the primary marker of an active star. For comparison with recent EW studies, we define a feature with positive EW as being in emission and negative EW as being in absorption. Previous studies such as

(1996); Hawley, Reid, & Tourtellot (2000); Gizis, Reid, & Hawley (2002) use a cutoff of 1.0 Å as the minimum EW at which one can unambiguously detect emission in a M dwarf. We measured 23 stars with 0.0 < EW < 1.0 Å and 14 stars with EW > 1.0 Å. Of the 23 low-emission objects, emission was confirmed by eye for only eight stars. In the remaining 15 low-emission stars, the Hα feature is too small to distinguish from the noise. We have decided to include only the eight stars where Hα can be confirmed by eye in our group of M stars with emission (dMe). Though this is a subjective way of establishing a minimum limit of detectability, it ensures that we follow only stars that are definitely in emission through our analysis. In Figure 2, the 22 dMe stars are plotted as filled circles. The 15 stars with questionable emission are plotted as open circles with crosses. We refer to these as dM(e) or intermediate dM stars, and keep track of their location throughout our analysis, in an attempt to deduce their true nature and assess the reliability of detecting emission in M dwarfs with EW < 1.0 Å. Finally the stars that were identified as having no Hα emission (dM) are plotted as crosses. We maintain this notation in all subsequent plots. Although some of the dMs may be dM(e) within our uncertainty, we are confident that none of the dM or dM(e) are dMe.

Figure 3 illustrates the fraction of stars in emission per half-spectral class in our sample (solid line) as compared to Hawley, Gizis, & Reid (1996, hereafter HGR - dashed line). Though the number of stars per bin is significantly less for our sample than for HGR the trend toward a higher fraction of dMe to dM stars per 0.5 spectral type is similar (and within the uncertainty) up to a spectral type of $\sim$ M4.5 where the number of stars in our sample drops precipitously. Only a small fraction of stars are in emission at early M spectral types in both samples.

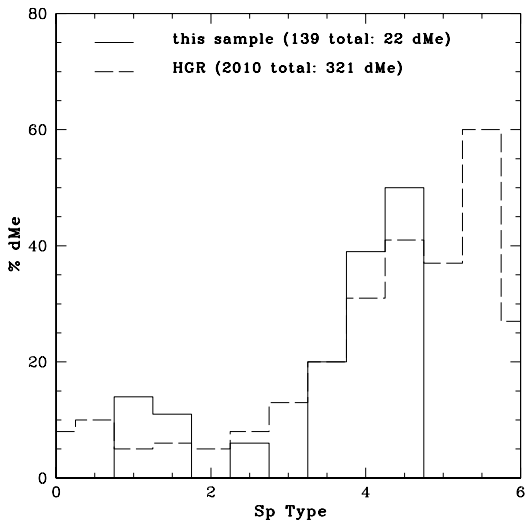

FIG. 3.— Ratio of dMe stars to the total number of M stars in each 0.5 spectral class bin. The solid line represents our sample, the dashed line indicates the HGR sample. There are 139 total stars in our sample and 2010 total stars in the HGR sample. As discussed in the text, our sample have very few stars later than type M4.5.

4.2. *Activity and Age*

In Figure 4 we divide the sample by spectral type into seven separate panels. The symbols are the same as given in Figure 2. The top panel contains the earliest spectral type (late K; previously classified as early M dwarfs based on low-resolution spectra) stars in the sample. The next five boxes are spectral types M0, M1, M2, M3, and M4 respectively. The last box contains all of the later type M dwarfs in our sample. The Hα EWs of the stars are plotted (in Å) versus the ages (in Gyr).

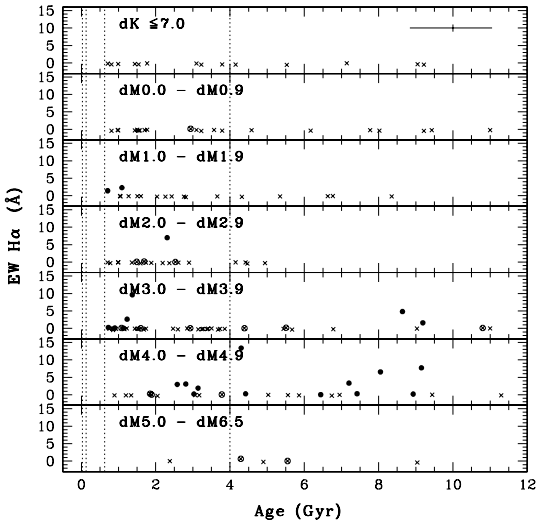

FIG. 4.— The EW Hα per 1.0 spectral type bin versus age for our sample. The filled circles represent the 22 dMe in our sample. The open circles with crosses represent the 15 intermediate dM(e) stars and finally the crosses, all at or below zero EW, are the remaining 102 inactive dMs. Vertical dotted lines indicate the ages derived for clusters observed in the PMSU study. Average error bars are given at the right hand side of the top panel. See text for detailed discussion.

The average error in age (largely a result of the errors in photometry and mass) is approximately $\pm$ 1.0 Gyr as shown at the right of the top panel. The actual average errors for the EWs are much smaller (formally $\sigma_{\mathrm{H}\alpha} = ^{+0.03}_{-0.02}$ Å) and arise primarily from the placement of the pseudo-continuum points. The four vertical dotted lines represent the ages of the clusters used in the HRT activity−age relation. The youngest clusters, IC2602 and IC2391, are both $\sim$ 30 Myr old, while the slightly older clusters NGC2516 and the Pleiades are grouped together at 125 Myr. The third line at 625 Myr is the age of the Hyades cluster and the final line at 4 Gyr is at the age of M67, the oldest cluster in their sample.

There are several important features that warrant discussion in this Figure. First, and not surprisingly, it appears that at early ages (< 4 Gyr), there are active M dwarfs in nearly every well-populated spectral type bin with the exception of M0. A large fraction of our dM(e) stars are located within this age range as well. HRT found that nearly every star in their youngest clusters was active above a certain threshold so it is not surprising that a large fraction of our active stars are apparently young.

However, the majority of our sample is quite old in comparison to the clusters studied by HRT. We have no stars as young as their four youngest clusters and have very few M dwarf stars that are even as young as

activity−age relation is well sampled; as expected, our sample will contribute important information on activity at relatively old ages. A large fraction of our stars are older than the oldest cluster (M67 at 4 Gyr) available for the cluster activity−age relation.

Another interesting aspect of Figure 4 is the striking lack of active stars with ages greater than 4 Gyr and spectral types earlier than M3. There are virtually no active M stars earlier than type M3 that are older than roughly 2 Gyr. Stars in our sample with spectral types M3 and later appear to remain active for much longer. Again this agrees qualitatively with the cluster results.

The next three figures (Figures 5-7) show M_V, $V-I$, and mass versus log(age) respectively. Table 4 lists the $V-I$, M_V, and mass values (columns 4-6) for the active (dMe and dM(e)) stars in Figures 5-7. The $V-I$ colors for the M dwarfs in our sample are from Smith (1997). We determined the M_V for the stars in our sample based on Reid & Hawley (1999) $4^{\rm th}$ order polynomial fit relating the M_V to the $V-I$ color of the star as

$$M_V = 3.98+1.437(V-I)+1.073(V-I)^2-0.192(V-I)^3. \quad (5)$$

This polynomial proves to be a good fit, in particular to stars with $0.85 < (V-I) < 2.85$. There is an abrupt discontinuity in the slope of M_V versus $V-I$ for dM stars at a $V-I \sim 2.9$ (dM4). Stars at this point have magnitudes $\pm$ 1.5 in M_V in either direction with the midpoint at $M_V \sim 13$. For stars with $V-I \sim 2.9$ in our sample, we assigned the midpoint value of $M_V \sim 13$ with errors of $\pm$ 1.5. For all other stars in Figures 5-7 the uncertainties in M_V, $V-I$, and mass are the size of the data points. For clarity, the uncertainties in age are given for only the active stars. The average age uncertainty for the rest of the points is $\pm$ 1 Gy.

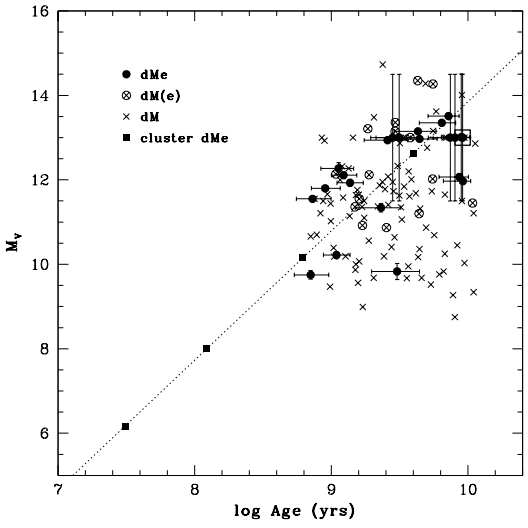

FIG. 5.— The M_V versus log(age) relation for our sample. The points are the same as in previous figures with the addition of the four solid squares representing the cluster ages from the PMSU study along with the corresponding empirical fit (dotted line). The open square denotes the location of LP133−373/374.

The M dwarf masses were determined using the relation from Delfosse et al. (2000):

$\log \frac{M}{M_\odot} = 10^{-3}[0.3 + 1.87(M_V)+$

$7.6140(M_V)^2 - 1.6980(M_V)^3 + 0.060958(M_V)^4], M_V \in$

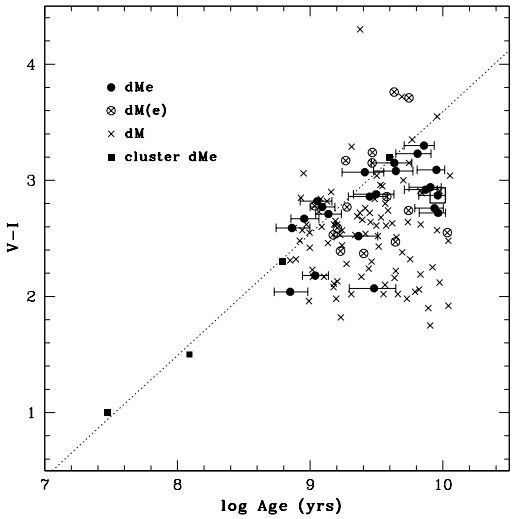

FIG. 6.— The $V-I$ versus log(age) relation for our sample. Symbols are the same as in Figure 5. The open square denotes the location of LP133−373/374.

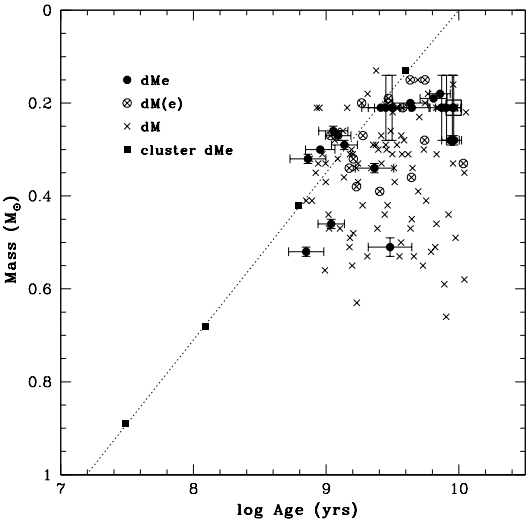

FIG. 7.— The M dwarf mass versus log(age) relation for our sample. Symbols are the same as in Figures 5 and 6. The open square denotes the location of LP133−373/374.

(6)

Figures 5-7 are directly comparable to the cluster results shown in HRT, and to Figure 11 ($V-I$ plot only) in Gizis, Reid, & Hawley (2002). We reproduce the cluster results on our plots with the dotted line connecting the four filled squares (representing the 4 unique Hα turn-off ages of the six clusters). The cluster age-activity relation identifies the dotted line as the suggested activity limit: stars that are fainter in absolute magnitude, redder in color, and lower in mass at a given age than the value of the relation (i.e. above the line in our plots) should be active, while stars below the line should be inactive. Results for our CPMB systems are shown with the same symbols as in previous plots.

Many of the dMe stars in our sample are more active than the cluster relation would predict. The same is

number of the dMe stars fall below the relation, indicating that with the larger age spread and the sampling of individual variations possible using our CPMB sample, the cluster relation is to simplistic. At the oldest ages we sample, near 10 Gyrs, the dMe stars are often bluer, more massive and, to a lesser extent, brighter than the cluster relation would predict. In other words, magnetic activity is lasting longer in these higher mass stars than is observed in clusters. The average errors in M_V (< 0.5 magnitudes), $V-I$ (< 0.1 magnitudes), and mass (< 0.1 $M_\odot$) cannot account for all of the discrepancy.

We note that one possible source of bias in our sample is the presence of a close, unresolved binary companion. In early M dwarfs, the induced synchronous (fast) rotation of such a system can increase the dynamo heating and produce strong emission even in old systems. Gizis, Reid, & Hawley (2002) point to a few M dwarfs in the D region of their Figure 5 as being active due to the presence of spectroscopically identified binary companions. Fischer & Marcy (1992) show that among binaries with M dwarf components, the incidence of detectable unresolved tertiary components is about 7%. Smith (1997) detected evidence of unresolved tertiary components (via anomalies in $BVRI$ colors) in about 10% of the 500 Luyten-Giclas pairs. Given that binaries comprise about 0.5-0.75 of the stars in the solar neighborhood (Abt 1988), one would expect a sample of single stars to be several times more seriously impacted by unresolved binary pairs than a wide binary sample is impacted by unresolved tertiary components.

To investigate this effect, Oswalt et al. (2004) report on time series photometric observations of all of our pairs which contain active M dwarf components in order to search for light variations in either the WD or main sequence components. Each pair receives at least a half night of observing time. So far, only one, LP133-373/374 (dM4e+DC, black open square in Figures 5-7) has shown any periodic variability that exceeds 2% in amplitude. The dMe component in this pair exhibits partial eclipses with a period of about 19.5 hours, suggesting that its enhanced activity is at least partially due to tidal interaction between two unresolved nearly identical dMe stars. The lightcurves of LP133-373/374 and other wide pairs will be published elsewhere. Nevertheless, the low incidence of short term photometric variability in the CPMB sample suggests that third components in, general, do not appear to account for most of the scatter seen in Figures 5-7.

An interesting finding, which again differs from the cluster results, is that for our binaries, not all M dwarfs that lie above the limiting relation are in emission (inactive M dwarfs are marked as crosses in the Figures). All (of the observed) cluster M dwarf stars that were redder (fainter, less massive) than the limiting relation had Hα in emission. This may indicate that stars in clusters are more uniform in their activity evolution than those in the field at the same age. However, again the possibility of unresolved companions, and/or differences in evolution between M dwarfs in clusters and M dwarfs in binary systems with a white dwarf may be causing unknown effects on the magnetic field generation in the M dwarf. As the driving mechanism behind the magnetic heating of the mid-M dwarfs is not well understood, there is no way of predicting the effect of different kinematical or residual orbital effects on such a mechanism. Evidently variables other than mass and rotation rate may influence the magnetic activity in such old systems. Also, we emphasize that the binaries are from a field star sample with consequent uncertainties in their individual evolution and properties, which contribute to the more complicated nature of their activity−age relation.

In summary, the general trend of lower mass (redder, fainter) stars remaining active longer than was predicted from the cluster results is confirmed. However, the scatter is larger, the activity is not ubiquitous, and the relation is not linear with log(age) for the ages older than 1 Gyr which we sample with our binaries.

5. M DWARF KINEMATICS

In this section we examine the kinematics of active and inactive M dwarfs for the sample of 161 M dwarfs in CPMB systems. The sample includes an additional 45 M dwarfs observed after the original investigation of Silvestri, Oswalt, & Hawley (2002, hereafter SOH). Twenty-two of these stars were excluded from the age-activity analysis in the previous section because we did not have photometry for their white dwarf companions and therefore could not determine their ages. However, they are included here because we do have good M dwarf data to determine their space motions. Table 5 gives the new velocity data for the sample, including the 45 WD+dM systems not presented in SOH. Columns 1-3 list the WD name assigned by Luyten, the R.A. and Decl. (coordinates are for equinox 1950). Columns 4-7 list the proper motion, the direction of proper motion, our measured radial velocity (v_r), and uncertainty in radial velocity (σ_{v_r}). Columns 8-15 give the UVW-space motions, their uncertainties, and the full space motion of each system. As with previous tables, a reference column (16) indicates the designation (dMe, dM(e), or dM) for each M dwarf. As in SOH, the space velocities are in a left-handed coordinate system.

The metallicity of the M dwarfs, determined by comparing CaH and TiO band strengths provides additional information on the population membership of the CPMB systems. Figure 8 shows the CaH2 versus TiO5 plot originally calibrated by Gizis (1997) to give a rough metallicity estimate for M dwarfs. Metal poor halo stars would lie below and to the right of the disk sequence represented by the bulk of the points plotted in the Figure. LP164−52 remains the only probable subdwarf in this sample. The rest appear to have solar-like metallicities which suggests that all but one of the 161 binaries are part of the Galactic disk population[6].

Figure 9 shows the U- versus V-velocity components of the space motion for the 161 binaries with good M dwarf spectra. The symbols are similar to those in previous figures, with dMe stars denoted by filled circles, dM(e) stars by open circles with crosses. The dM stars are now represented by open circles for clarity (they were denoted by crosses in previous Figures). As expected from the metallicity results, the stars are nearly all contained within the velocity contours of the Galactic disk (thin and thick components, including the eclipsing M dwarf, LP133−373 at [+19.0, −9.0]). Except for a few obvious outliers (the potential subdwarf,

[6] The two objects in the upper right hand portion of Figure 3 of SOH have since been reobserved with higher quality spectra. The new data indicate better agreement with the rest of the sample in

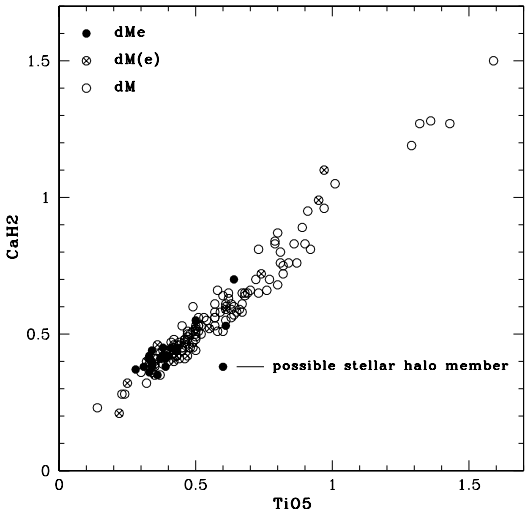

FIG. 8.— The CaH2 versus TiO5 relation for 161 M dwarfs in binary systems. The bandpasses for CaH2 and TiO5 are 6814-6846 Å and 7126-7135 Å, respectively. Symbols are the same as in Figures 5-7 except the dMs are now shown as open circles. We find only one potential subdwarf system, LP164-52.

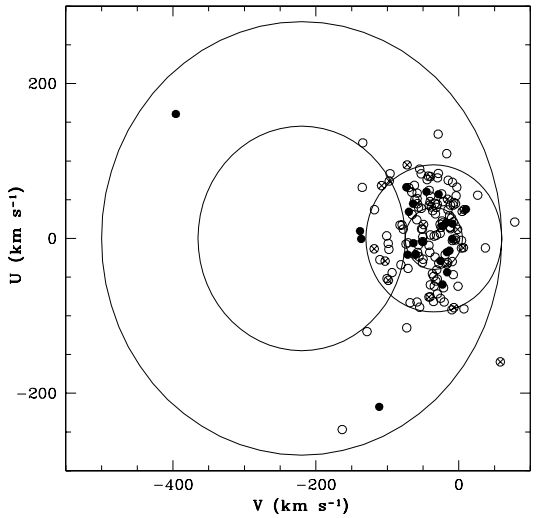

FIG. 9.— The U versus V velocity distribution of 161 binary systems with measured Hα EWs and radial velocities. The symbols are the same as in Figure 8. The ellipsoids plot the 1σ (inner) and 2σ (outer) contours for the Galactic thick-disk and stellar halo populations, respectively. Typical errors are approximately $\pm$ 10 km s^{-1}.

LP164−52 at [−0.7,−136.6], HZ 43B, LP219−78, and LP205−28), the active stars have lower average velocities and are more closely confined to the thin disk, in agreement with previous results (Reid, Hawley, & Gizis 1995; Hawley, Gizis, & Reid 1996). The marginally active dM(e) stars, in contrast, are more closely aligned with the higher velocity, inactive dM stars. The plot also reveals a few additional high velocity systems compared to the earlier SOH results. The spectra for these high velocity systems are of equivalent quality to the rest of the spectra and there are no obvious systematic errors which would result in velocities that are larger than the average of the distribution. Their large velocities are likely a result of being part of the high velocity tail of the thin or thick disk population of the Galaxy. The additional data shown in Figure 9 support the conclusions of SOH that the high velocity white dwarf stars in this sample are not part of a dark matter halo, in contrast to the suggestion of Oppenheimer et al. (2001a).

6. CONCLUSIONS

We have determined the ages for 139 M dwarf stars in CPMBs to an accuracy of $\pm$ 1 Gyr and have extended the chromospheric activity−age relation to ages much older than the oldest open cluster used in previous work. As found in previous work, lower mass (redder, later spectral type) M dwarfs are more likely to be active at old ages than higher mass M dwarfs. However, we have demonstrated that our activity−age results for M dwarfs in wide binary systems depart from the log-linear relations seen in cluster M dwarfs. Neither the uncertainties in the age estimates for the binary M dwarfs nor the uncertainties in cluster age estimates can account for the disparity between the two relations. Active M stars of a given age in our sample are found at higher mass, bluer color and brighter absolute magnitude than predicted from the cluster results.

In addition, the activity in our CPMB M dwarfs is not mass as is found to be the case for M dwarfs in clusters. Evidently the magnetic activity evolution in clusters is more uniform than in these field binaries, at least for ages < 4 Gyr. The same activity behavior we observe may be present in older clusters, which are as yet too faint to be observed. It is not clear what mechanism would selectively allow for emission at a particular age in some old M dwarf stars while prohibiting it in others of the same mass and spectral type at the same age. Possible explanations for the discrepancy include unresolved close companions that induce fast rotation in some M dwarfs even at old ages, or as yet unknown evolutionary effects due to the presence of a companion white dwarf (albeit at a large distance from the M dwarf).

We have successfully extended the activity−age relations to ages several Gyr older than the cluster relations, but it is clear that more work needs to be done to increase the number of old M dwarf stars for which accurate ages can be determined. For a more complete picture of old M stars, work must also be done to extend this relation to later spectral types, as our study is not well sampled at types later than M4.5. Recent studies (West et al. 2004) show that magnetic activity is strongly correlated with spectral type in large samples of disk stars, and also depends on distance from the Galactic plane, another age-dependent factor.

In the context of previous work, our analysis suggests that nearly all of our high velocity common proper motion binary WDs are part of a rotating component and have kinematics which resemble the high velocity tail of the Galaxy's disk population as found in SOH. Also, the M dwarf stars in our sample exhibit metallicities indicative of the thick disk component of the Galaxy, just as Reid, Sahu, & Hawley (2001) demonstrated with their large sample of M dwarf stars. Our study of WD+dM systems demonstrates that the active M dwarfs exhibit mostly thin disk kinematics, as expected of a

dwarf companions provide essential confirmation of population membership.

This work was supported by the NASA Graduate Researchers Program Grant NGT 200415 (NMS); NFS AST02-05875 (NMS, SLH); A Grant-in-Aid of Research from the National Academy of Sciences administered by Sigma Xi, The Scientific Research Society (NMS); NASA Grant Y701296 (TDO); and NSF Grant AST 0206115 (TDO).

REFERENCES

Abt, H. A. 1988, Ap&SS, 142, 111
Barry, D. C. 1988, ApJ, 334, 436
Bergeron, P., Ruiz, M.-T., & Leggett, S. 1997, ApJS, 108, 339
Bergeron, P., Saumon, D., & Wesemael, F. 1995, ApJ, 443, 764
Boss, A. P. 1987, ApJ, 319, 141
Boss, A. P. 1988, in Comments on Astrophysics, Vol. 12, 169
Byrne, P. B. 1993a, A&A, 272, 495
Byrne, P. B. & Doyle, J. G. 1990, A&A, 238, 221
Chabrier, G. 1993, ApJ, 414, 695
Dawson, P. C. 1986, ApJ, 311, 984
Delfosse, X., Forveille, T., Ségransan, D., Beuzit, J.-L., Udry, S., Perrier, C., & Mayor, M. 2000, A&A, 364, 217
Ding, M. D. & Fang, C. 2001, MNRAS, 326, 943
Fischer D. A. & Marcy G. W. 1992, ApJ, 396, 178
Giclas, H. L., Burnham, R., & Thomas, N. G. 1971, in Lowell Proper Motion Survey, Northern Hemisphere: The G−Numbered Stars (Flagstaff: Lowell Observatory)
Giclas, H. L., Burnham, R., & Thomas, N. G. 1978, Lowell Observatory Bulletin, 8, 89
Gizis, J. E. 1997, AJ, 113, 806
Gizis, J. E., Reid, I. N., & Hawley, S. L. 2002, AJ, 123, 3356
Hawley, S. L. et al. 2002, AJ, 123, 3409
Hawley, S. L., Gizis, J. E., & Reid, I. N. 1996, AJ, 112, 2799 **HGR**
Hawley, S. L., Reid, I. N., & Tourtellot, J. G. 2000, in La Palma Conf. on Very Low Mass Stars and Brown Dwarfs in Stellar Clusters and Associations, eds. R. Rebolo & M. R. Zapatero-Osorio (Cambridge: Cambridge University Press), 109 **HRT**
Hawley, S. L., Tourtellot, J. G., & Reid, I. N. 1999, AJ, 117, 1341
Hernanz, M., García-Berro, E., Isern, J., Mochkovitch, R., Segretain, L., & Chabrier, G. 1994, ApJ, 434, 652
Iben, I. & Laughlin, G. 1989, ApJ, 341, 312
Isern, J., Hernanz, M., Mochkovitch, R., & García-Berro, E. 1991, A&A, 241, 291
Isern, J., Mochkovitch, R., García-Berro, E., & Hernanz, M. 1997, ApJ, 485, 308
Kirkpatrick, J. D., Henry, T. J., & McCarthy, D. W. 1991, ApJS, 77, 417
Koester, D. 1987, ApJ, 322, 852
La Bonte, A. E. 1970, in IAU Colloq. 7, Proper Motions, ed. W. J. Luyten (Minneapolis: University of Minnesota Minneapolis Press), 26
Lamb, D. Q. & Van Horn, H. M. 1975, ApJ, 200, 306
Liebert, J., Dahn, C. C., & Monet, D. G. 1988, ApJ, 332, 891
Luyten, W. J. 1963, in Proper Motion Survey with the Forty-Eight Inch Telescope (Minneapolis: University of Minnesota Minneapolis Press)
Luyten, W. J. 1969, in Proper Motion Survey with the Forty-Eight Inch Telescope (Minneapolis: University of Minnesota Minneapolis Press)
Luyten, W. J. 1974, in Proper Motion Survey with the Forty-Eight Inch Telescope (Minneapolis: University of Minnesota Minneapolis Press)
Luyten, W. J. 1979, in Proper Motion Survey with the Forty-Eight Inch Telescope (Minneapolis: University of Minnesota Minneapolis Press)
Martín, E. L. & Ardila, D. R. 2001, ApJ, 121, 2758
Mochkovitch, R. 1983, A&A, 122, 212
Noyes, R. W., Hartmann, L. W., Baliunas, S. L., Duncan, D. K., & Vaughan, A. H. 1984, ApJ, 279, 763
O'Neal, D., Neff, J. E., & Saar, S. H. 1998, ApJ, 507, 919
Oppenheimer, B., Hambly, N. C., Digby, A. P., Hodgkin, S. T., & Saumon, D. 2001a, Science, 292, 698
Oswalt, T. D., Hintzen, P. M., & Luyten, W. J. 1988, ApJS, 66, 391
Oswalt, T. D., Rudkin, M. A., Johnston, K., Kissinger, J., & Menezes, K. 2004, in ASP Conf. Proc. of the 14th European Workshop on White Dwarfs, eds. D. Koester & S. Jordan (Dordrecht: Kluwer), in press.
Oswalt, T. D., Sion, E. M., Hintzen, P. M., & Liebert, J. W. 1991, in Proc. of European Workshop 7, White Dwarfs, eds. G. Vauclair & E. M. Sion (ASP), 379
Oswalt, T. D. & Smith, J. A. 1995, in Proc. of the European Workshop 9, White Dwarfs, eds. by D. Koester & K. Werner (Berlin: Springer-Verlag), 24
Oswalt, T. D., Smith, J. A., Shufelt, S., Hintzen, P. M., Leggett, S. K., Liebert, J., & Sion, E. M. 1993, in Proc. of the European Workshop 8, White Dwarfs: Advances in Observation and Theory, ed. M. A. Barstow (Dordrecht: Kluwer), 419
Oswalt, T. D., Smith, J. A., Wood, M. A., & Hintzen, P. 1996, Nature, 382, 692
Pettersen, B. R., Lambert, D. L., Tomkin, J., Sandmann, W. H., & Lin, H. 1987, A&A, 183, 66
Pettersen, B. R. & Hawley, S. L. 1989, A&A, 217, 187
Pringle, J. E. 1989, MNRAS, 239, 361
Reid, I. N. 1996, AJ, 111, 2000
Reid, I. N. & Gizis, J. E. 1998, AJ, 116, 2929
Reid, I. N. & Hawley, S. L. 1999, AJ, 117, 343
Reid, I. N., Hawley, S. L., & Gizis, J. E. 1995, AJ, 110, 1838
Reid, I. N., Hawley, S. L., & Mateo, M. 1995, MNRAS, 272, 828
Reid, I. N., Sahu, K. C., & Hawley, S. L. 2001, ApJ, 559, 942
Salaris, M., García-Berro, E., Hernanz, M., Isern, J., & Saumon, D. 2000, ApJ, 544, 1036
Segretain, L., Chabrier, G., Hernanz, M., García-Berro, E., Isern, J., & Mochkovitch, R. 1994, ApJ, 434, 641
Silvestri, N. M., Oswalt, T. D., Wood, M. A., Smith, J. A., Reid, I. N., & Sion, E. M. 2001, AJ, 121, 503
Silvestri, N. M., Oswalt, T. D., & Hawley, S. L. 2002, AJ, 124, 1118 **SOH**
Skumanich, A. 1972, ApJ, 171, 565
Smith, J. A. 1997, Ph.D. thesis, Florida Institute of Technology
Smith, J. A. & Oswalt, T. D. 1995, in Proc. of the ESO Workshop, The Bottom of the Main Sequence−and Beyond, ed. C. G. Tinney (Berlin: Springer-Verlag), 113
Soderblom, D. R., Duncan, D. K., & Johnson, D. R. H. 1991, ApJ, 375, 722
Stauffer, J. R., Giampapa, M. S., Herbst, W., Vincent, J. M., Hartmann, L. W., & Stern, R. A. 1991, ApJ, 374, 142
Weidemann, V. 2000, A&A, 363, 647
West, A. A., Hawley, S. L., Walkowicz, L. M., Covey, K. R., Silvestri, N. M., Raymond, S. N., Harris, H. C., Munn, J. A., & McGehee, P. 2004, AJ, 128, 426
Wilson, O. C. 1966, ApJ, 144, 695
Wood, M. A. 1990, Ph.D. thesis, The University of Texas at Austin
Wood, M. A. 1992, ApJ, 386, 539
Wood, M. A. & Oswalt, T. D. 1998, ApJ, 497, 870

TABLE 1
Complete M Dwarf−White Dwarf Wide Binary Target List.

Identifier (Sp.1/Sp.2) (1)	R.A. (B1950) (2)	Decl. (B1950) (3)	$V1$ (4)	Sp.1[a] (5)	$V2$ (6)	Sp.2[a] (7)	Site (8)	U.T. (mm/yy) (9)	Exp. (sec) (10)	μ ($''$/yr) (11)	Θ_μ (deg) (12)	Pos. (deg) (13)	Sep. ($''$) (14)
LP349−14/13	00:22:06	27:24:00	13.40	dM	16.86	DB	APO	06/01	300	0.12	90	305	113
G158−77/78	00:23:28	-10:53:30	13.47	sdM1	16.23	DA	APO	09/00,06/01	300	0.27	160	127	90
G171−B10A/B	00:23:53	38:52:24	15.97	DA	15.26	dM5	APO	09/00	900	0.20	132	202	25
L170−14A/B	00:27:30	-54:58:00	14.84	dM3.5	16.23	DA	CTIO	01/02	900	0.36	240	327	3
G218−8/7	00:38:30	55:33:42	14.1	DQ5	14.02	dM	APO	09/00	1000	0.32	103	246	11
LP825−712/713	00:40:36	-22:02:00	15.7	sdM1	18.0	DA3	APO	09/01	900	0.50	83	50	23
LP242−11/12	00:52:30	38:32:00	13.80	dM0	18.29	DC	APO	09/00,09/01	300	0.50	242	56	22
LP1−169/170	01:01:00	86:40:00	15.2	dM1	16.7	DQ	APO	12/00	450	0.13	73	326	7
Wolf 53/LP79−8	01:02:51	61:04:18	14.87	dM5	18.22	DC	APO	09/00	800	0.48	137	302	9
LP586−65/64	01:04:14	01:32:42	17.28	DA	18.35	dM5	APO	09/01	1800	0.25	89	213	175
LP587−44/45	01:19:15	-00:26:30	16.42	DB	18.07	sdM5	APO	09/01	2400	0.19	230	264	9
LP587−54/53	01:20:42	-02:24:48	12.62	dM2	17.48	DC	APO	10/00	150	0.22	79	199	44
LP29−148/149	01:23:48	73:12:00	16.8	DA	17.0	dM5	APO	09/01	1200	0.23	290	43	69
G34−48/49	01:42:31	23:02:48	13.08	sdM3	16.9	DC4	APO	10/00	240	0.32	112	60	24
LP352−31/30	01:45:06	21:32:00	15.41	dM5	18.32	DA	APO	10/00	600	0.20	80	270	13
G244−37/36	01:48:12	64:11:24	11.39	dM2	13.96	DA6	APO	12/00	180	0.29	129	178	16
G71−B5A/B	01:50:31	08:56:42	14.21	dM4	17.22	DZ	APO	10/00	800	0.10	154	311	13
G272−B2A/B	01:58:32	-16:00:36	14.71	DBA	16.02	dM3	APO	09/01	600	0.13	81	164	7
LP885−23/22	02:04:51	-30:38:30	14.14	dM5	16.92	DA	CTIO	01/02	160	0.25	124	313	73
LP245−17/18	02:17:21	37:33:48	13.8	dM5	18.1	DA	APO	12/00	180	0.35	102	90	2
LP590−143/142	02:25:52	00:24:30	18.08	DA	17.85	dM5	APO	10/00	1500	0.11	155	316	73
LP530−22/21	02:28:34	07:57:24	17.38	DC	17.77	dM5	APO	02-09/01	2700	0.35	134	158	23
LP197−55/56	02:46:12	43:24:00	18.78	DC	18.40	dM4.5e	APO	10/01	2400	0.26	71	69	10
LP411−23/22	02:52:54	20:54:00	17.58	DA	18.78	dM4.5	···	···	···	0.25	118	40	12
LP355−11/10	02:57:42	24:42:00	16.81	dM5	18.52	DC	APO	02/01	1800	0.18	124	239	138
LP472−38/39	03:17:18	11:24:00	14.55	dM0	19.05	DQ	APO	12/00	450	0.18	192	23	17
LP355−64/65	03:19:30	26:59:00	11.5	dM1	17.6	DA	APO	10/00	100	0.21	113	98	278
LP31−139/140	03:24:30	73:15:00	17.5	DC7	16.48	dM4.5e	APO	12/00	1500	0.43	141	9	12
LP356−87/88	03:25:00	26:21:00	13.62	dM	17.66	DA	APO	10/00,02/01	600	0.18	120	309	6
LP888−64/63	03:26:45	-27:18:36	13.9	DA	15.3	sdM3	CTIO	02/02	600	0.83	63	227	7
LP773−12/11	03:31:48	-16:05:00	15.03	dM5	18.52	DC	APO	10/00	600	0.32	80	235	6
LP31−276/277	03:54:36	70:47:00	12.96	dM0	18.37	DC	APO	01/01	400	0.17	74	185	9
LP889−21/20	03:58:06	-32:06:00	15.72	dM5	18.63	DC	CTIO	01/02	480	0.21	117	276	10
40 Eri−A	04:13:03	-07:44:06	···	dG8	···	···	···	···	···	4.08	213	105	82
40 Eri−C/B	04:13:03	-07:44:06	4.35	dM5e	9.51	DA4	···	···	···	4.08	213	105	82
LP415−1/2	04:17:12	19:47:00	16.33	dM5	17.88	DA	APO	01-02/01	1600	0.17	216	138	30
LP775−52/53	04:19:26	-16:07:06	12.56	dM0	17.42	DA	APO	10/00	200	0.35	112	142	12
G175−34A/B	04:26:50	58:53:18	11.88	dM5	12.39	DC5	APO	12/00	60	2.37	146	82	6
HZ 9A/B	04:29:24	17:38:00	13.95	DA2	18.0	dM1	APO	01-02/01	1800	0.12	110	103	13
BD+26°730/LP358−52A	04:32:54	26:56:00	18.32	DA	18.75	DC	APO	12/00	2700	0.11	108	118	1
LP358−52B	04:32:54	26:56:00	18.0	sdM1	···	···	APO	12/00	2700	0.11	108	118	1
LP891−13/12	04:43:18	-27:32:00	15.41	dM4.5e	16.69	DQ	CTIO	01/02	400	0.24	246	62	49
G86−B1A/B	05:18:26	33:19:12	14.26	dM5	15.98	DAe	APO	10/00	900	0.18	113	203	9
LP120−25/26	05:51:48	56:02:00	18.80	sdM0	18.1	DA	APO	01/01	1800	0.14	115	300	7
LP120−27	05:51:48	56:02:00	14.0	dK	···	···	APO	01/01	500	0.14	115	300	7
LP159−33/32	05:51:59	46:50:54	17.13	dM5	15.47	DC	APO	01-02/01	1800	0.54	179	219	12
LP779−19/20	06:04:18	-19:50:00	17.22	DQ	18.38	dM5	CTIO	01/02	1800	0.23	108	53	43
G105−B2A/B	06:25:01	10:02:30	13.16	dM2	16.48	DCZ6	APO,CTIO	01/01,01/02	400	0.10	151	310	127
LP600−42/43	06:28:08	-02:03:42	15.36	DA	15.56	dM5	APO,CTIO	01/01,01/02	800	0.25	214	307	4
LP205−27/28	06:41:50	43:48:36	15.53	DA	18.41	dM5	APO	01/01	2400	0.12	176	107	143
G87−29/28	07:06:52	37:45:24	15.60	DQ8	14.60	dM4.5e	APO	01/01	540	0.44	222	224	15
LP422−6/7	07:09:18	19:24:00	17.19	DA	16.24	dM5	APO	01/01	1200	0.10	147	179	284
LP5−74/73	07:26:00	82:44:00	15.08	dM0	18.73	DC	APO	01/01	500	0.18	76	279	5

TABLE 1 — *Continued*

Identifier (Sp.1/Sp.2) (1)	R.A. (B1950) (2)	Decl. (B1950) (3)	$V1$ (4)	Sp.1[a] (5)	$V2$ (6)	Sp.2[a] (7)	Site (8)	U.T. (mm/yy) (9)	Exp. (sec) (10)	μ ($''$/yr) (11)	Θ_μ (deg) (12)	Pos. (deg) (13)	Sep. ($''$) (14)
LP207−7/8	07:26:06	39:17:00	15.81	DA	15.12	dM5	APO	12/00	900	0.12	186	50	44
G107−69/70	07:27:02	48:19:06	13.52	sdM5	14.65	DC9	APO	01/01	400	1.34	191	155	105
LP783−3/2	07:38:02	-17:17:24	13.05	DZQ6	16.67	dM	APO	01/01	1200	1.26	117	276	21
LP366−2/3	07:41:37	24:50:24	15.29	dM5	16.52	DA	APO	01-04/01	1200	0.10	260	86	101
LP208−33/32	08:04:18	44:40:00	15.40	dM5	17.77	DA	APO	01/01	600	0.10	200	280	18
LP664−16/15	08:06:30	-04:23:00	12.98	dM2	18.26	DC	APO	01/01	300	0.12	182	220	20
LP163−120/121	08:07:24	48:25:00	15.61	dM2	18.10	DA8	APO	01/01	800	0.14	79	40	11
G111−72/71	08:16:47	38:44:18	13.12	sdM2	16.55	DAZ7	APO	01/01	400	0.38	212	258	34
L186−119/120	08:20:42	-58:32:00	16.58	DA	15.85	dM5	CTIO	01/02	···	0.20	289	85	21
LP164−52/51	08:42:48	49:37:00	18.31	DA	19.30	dM0	APO	01/01	2400	0.31	159	296	5
LP844−26/25	08:51:42	-24:36:00	18.07	DC	18.03	dM4.5e	APO	01/01	2400	0.64	78	270	18
LP60−359A/B	08:52:24	63:03:00	15.31	DA9	16.94	dM5e	APO	12/00	2700	0.11	110	65	36
LP90−70/71	08:55:40	60:28:18	16.34	DBQ	15.68	dM	APO	01/01	800	0.53	216	60	44
LP845−9/8	08:58:42	-22:02:00	14.68	dM2	18.37	DC	APO	01/01	540	0.19	319	288	5
LP60−177/178	08:59:30	68:17:00	15.14	dM1	18.71	DA	APO	01-02/01	2700	0.16	215	3	12
LP313−12/13	09:04:30	27:49:00	17.97	DA	17.47	dM4.5e	APO	01/01	1800	0.13	160	36	24
LP313−16/15	09:06:18	29:42:00	15.74	DA3	15.61	dM5	APO	01/01	800	0.14	237	324	11
LP36−141/142	09:06:48	72:45:00	18.59	DZ	19.31	dM5	···	···	···	0.12	195	143	11
LP369−15/14	09:08:51	22:40:06	18.28	DA	19.32	dM1	···	···	···	0.11	120	277	200
LP60−237/236	09:11:24	65:09:00	13.61	dM1	17.32	DC	APO	01/01	300	0.14	241	310	6
LP487−25/26	09:16:00	11:11:00	18.38	DC	17.37	dM4.5e	APO	01/01	1800	0.35	235	77	25
LP787−26/25	09:18:30	-17:16:00	17.78	DA	17.84	dM4.5e	APO,CTIO	01/01,02	2400	0.20	323	253	13
G117−B15A/B	09:21:13	35:29:48	15.45	DAV4	15.99	dM2	APO	01/01	1200	0.14	264	126	15
G161−36/37	09:26:51	-03:57:00	14.76	DA	15.21	dM5	APO	01/01	600	0.27	274	180	19
LP668−10/9	09:37:24	-09:32:00	15.86	dM4.5e	17.25	DC	APO	01-02/01	1800	0.25	157	353	13
LP488−20/19	09:37:42	09:21:00	16.82	dM	18.09	DC9	APO,CTIO	01/01,02	1800	0.26	255	241	9
LP370−41/40	09:41:00	22:34:00	17.14	DA	17.82	dM	APO	04/01	1800	0.12	201	190	13
G117−B11A/B	09:43:23	33:05:18	15.10	dM5	17.12	DA	APO	01/01	500	0.14	133	11	14
LP62−34A/35	10:04:36	66:34:00	12.29	dM	14.67	DZ	APO	01/01	900	0.21	224	312	56
LP62−34B	10:04:36	66:34:00	16.0	DC	···	···	APO	01/01	900	0.21	224	180	3
LP847−41/40	10:10:18	-23:58:00	16.90	dM5	18.29	DAZ	CTIO	01/02	700	0.18	312	315	17
CD−18°3019/LP791−55	10:43:30	-18:50:00	11.04	dM0e	15.49	DQ9	APO	01/01	120	1.98	250	356	7
LP214−11/10	10:54:24	41:59:00	13.02	dM1.5	18.62	DC	APO	12/00	1800	0.13	210	318	189
LP317−25/26	10:54:24	30:30:00	14.98	dM0	17.89	DC	APO	01/01	500	0.16	270	8	158
LP731−37A/B	10:59:06	-11:57:00	18.3	WD	17.5	dM5	CTIO	02/02	1800	0.40	254	229	2
LP551−66/67	11:04:30	04:25:00	15.4	DA	17.7	sdM5	APO	02/01	2400	0.19	177	188	3
LP214−39/38	11:05:12	41:16:00	11.86	dM1	16.25	DC	APO	01/01	200	0.21	275	197	11
LP672−1/2	11:05:30	-04:53:00	13.10	DA3	12.60	dM6	APO	01/01	220	0.44	184	160	279
CD−25°8487/LP849−5	11:07:00	-25:43:00	8.66	sdM0	17.64	DC	CTIO	01/02	2	0.25	106	181	100
LP373−85/84	11:08:48	25:35:00	17.16	dM	19.05	DCZ	APO	02/01	1800	0.24	266	309	72
LP792−6/5	11:11:30	-18:47:00	15.73	dM5	18.33	DC	APO	02/01	1200	0.25	300	215	26
LP552−48/49	11:20:54	07:18:00	10.35	dM1	17.49	DC	APO	02/01	120	0.20	110	113	24
LP906−23/24	11:20:54	-32:07:00	16.46	dM5	18.44	DA7	CTIO	01/02	600	0.24	282	121	19
LP906−34/33	11:32:54	-29:53:00	14.45	dM5	15.50	dM5	CTIO	01/02	400	0.16	227	347	4
LP906−35A/B	11:32:54	-29:53:00	17.41	DA7	17.8	dM	CTIO	01/02	1800	0.16	227	188	52
LP493−16/15	11:33:48	08:19:00	13.84	dM	17.37	DZ	APO	02/01	500	0.25	245	210	6
G148−7/6	11:43:21	32:06:12	13.73	DA3.5	14.05	dM5	APO	01/01	300	0.28	203	271	9
LP375−51/50	11:47:46	25:35:18	15.66	DA5	15.50	dM2	APO	02/01	1500	0.30	252	252	36
LP493−61/60	11:48:48	13:11:00	14.16	dM	19.01	DC	APO	02/01	500	0.21	182	252	44
LP129−587/586	11:48:48	54:28:00	16.65	DA5	16.41	dM5	APO	02/01	1200	0.25	264	182	35
LP673−42A/B	11:50:43	-07:05:36	11.96	dM2	19.0	DC	APO	02/01	300	0.54	198	110	9
ESO440−55A/B	12:04:03	-31:20:30	19.12	DZ7	19.91	dM5	CTIO	01/02	···	0.22	273	···	5
LP674−29/CD−5°3450	12:09:48	-06:05:00	···	···	···	···	CTIO	01/02	1800	0.44	220	102	202
LP216−75/74	12:11:06	39:18:00	16.0	dM0	16.5	DA	APO	02/01	1200	0.13	302	250	15

TABLE 1 — *Continued*

Identifier (Sp.1/Sp.2) (1)	R.A. (B1950) (2)	Decl. (B1950) (3)	$V1$ (4)	Sp.1[a] (5)	$V2$ (6)	Sp.2[a] (7)	Site (8)	U.T. (mm/yy) (9)	Exp. (sec) (10)	μ ($''$/yr) (11)	Θ_μ (deg) (12)	Pos. (deg) (13)	Sep. ($''$) (14)
LP554−64/65	12:14:18	03:14:00	13.28	sdM3	14.9	DA	APO	01/01	300	0.70	293	190	2
LP320−644/643	12:15:06	32:22:00	15.01	dM	16.99	DC7	APO	02/01	900	0.26	234	330	6
LP435−58/59	12:20:24	19:06:00	17.26	DA	16.79	dM	APO	02-03/01	1800	0.19	268	90	22
LP795−13/14	12:22:48	-16:50:00	18.19	DA	17.18	dM5	APO	01/01	1800	0.12	211	137	28
LP495−176/177	12:30:36	12:16:00	16.52	dM	19.24	DC	APO	02/01	1500	0.16	284	165	8
LP321−206/205	12:30:42	26:22:00	19.39	DC	18.63	dM	APO,CTIO	04/01,01/02	3000	0.15	263	3	38
LP321−396/397	12:38:20	28:13:48	17.40	DA	19.19	dM4.5e	···	···	···	0.13	259	173	7
LP20−406/407	12:40:30	75:26:00	16.2	DA4	17.6	dM	APO	03/01	1800	0.23	266	129	6
LP321−458/459	12:43:34	30:19:54	18.5	DAB	19.5	dM	···	···	···	0.12	173	90	2
G61−16/17	12:44:44	14:58:24	13.51	sdM2	15.82	DA5	APO	01-04/01	300	0.43	298	47	25
LP497−29/30	13:11:30	11:14:00	17.42	dM4	18.64	DA	APO	04-06/01	1800	0.24	207	187	37
LP910-16/17	13:04:42	-27:47:00	···	dM	···	WD	CTIO	01/02	1200	0.10	54	231	115
HZ 43A/B	13:14:00	29:22:00	12.68	DA1	13.0	dM	APO,CTIO	01/01,01/02	300	0.16	240	280	3
LP617−34/35	13:17:42	-02:08:00	15.11	dM5	18.84	DC	APO	01-04/01	900	0.19	159	103	23
G14−58/57	13:27:40	-08:18:48	12.33	DA4	14.32	dM5e	APO	01/01	400	1.24	247	160	504
LP21−153/152	13:30:00	79:20:00	16.7	dM0	17.0	DA	APO	02/01	2700	0.10	290	265	4
LP798−13/14	13:34:18	-16:04:00	15.33	DA3	13.76	dM5e	APO	01/01	400	0.12	246	242	14
LP738−42/43	13:34:48	-11:48:00	14.93	dM5	18.10	DC	APO	02/01	1200	0.19	199	19	18
LP498−26/25	13:36:45	12:23:48	14.72	DB3	14.02	dM4	APO	02/01	400	0.19	134	307	87
LP380−6/5	13:45:44	23:50:00	15.64	DC9	15.41	dM4	APO	04/01	900	1.48	276	231	188
LP219−77/78	13:48:18	41:48:00	17.20	DA	17.59	dM5	APO	04/01	2400	0.14	160	98	8
LP856−54/53	13:48:30	-27:19:00	12.59	dM3	15.20	DA6	APO	02/01	600	0.24	199	233	9
LP439−180/179	14:00:42	16:04:00	17.38	dM0	18.33	DA	APO	04/01	1800	0.08	167	238	31
LP133−373/374	14:02:24	50:36:00	15.31	dM5e	18.42	DC	APO	02/01	1200	0.20	308	122	5
LP799−73/74	14:09:36	-18:29:00	17.12	DC	16.41	dM4.5	APO	03/01	1200	0.19	133	119	52
LP66−587/586	14:16:06	63:18:00	15.86	dM0e	17.49	DA	APO	02/01	1500	0.09	140	356	8
G200−40/39	14:25:59	54:01:00	11.92	sdM	15.06	DBA4	APO	02/01	400	0.39	294	349	39
LP621−35/36	14:50:00	-00:39:00	···	dM	···	WD	CTIO	01/02	1800	0.19	147	7	9
LP135−154/155	15:10:34	56:36:12	16.33	DA6	15.85	dM	APO	02/01	1500	0.38	217	86	18
LP223−13/14	15:25:30	43:23:30	16.47	DA	18.40	dM5	APO	03/01	2400	0.14	186	119	64
LP176−59/60	15:33:12	46:59:00	17.57	dM5	18.23	DC9	APO	03/01	1800	0.51	296	71	85
LP743−24/25	15:39:12	-13:47:00	18.74	DC	17.81	dM3	APO	03/01	2400	0.20	314	218	7
L480−84/85	15:41:54	-38:10:00	14.00	dM3	15.23	DA	CTIO	01/02	120	0.09	162	261	10
LP916−27/26	15:42:18	-27:30:00	15.38	DB4	15.18	dM5	APO	06/01	900	0.24	235	330	52
LP42−195/196	15:50:00	71:41:00	17.3	dM	19.5	DA	APO	02-06/01	3600	0.14	4	193	27
LP42−197	15:50:00	71:41:00	19.8	dM5	···	···	APO	02-06/01	3600	0.14	4	280	4
LP684−1/2	15:54:00	-04:41:00	···	dM	···	WD	CTIO	01/02	780	0.32	244	202	5
G152−B4A/B	15:55:22	-08:59:30	14.95	DA5	14.45	dM5	APO	02/01	600	0.12	198	295	10
L266−195/196	16:23:00	-54:05:00	11.55	dM1	15.35	DA5e	CTIO	01/02	100	0.08	12	4	39
LP101−15/16	16:33:30	57:15:00	12.91	dM5e	15.05	DQ8	APO	09/00	600	1.62	319	23	26
LP505−43/44	16:35:00	11:16:00	14.70	dM	18.80	DC	APO	09/00	400	0.17	159	77	60
LP686−33/32	16:56:12	-06:11:00	15.55	dM5	17.21	DC9	APO	09/00	600	0.35	111	211	110
LP387−37/36	17:03:54	26:10:00	12.16	dM	17.17	DC7	APO	09/00	···	0.28	185	359	19
Wolf 672A/B	17:16:05	02:00:12	14.36	DA6	14.05	dM5	APO	09/00	400	0.50	232	137	13
LP101−409/410	17:16:06	59:51:00	13.01	dM1	13.68	dM0	APO	06/01	600	0.18	355	9	72
LP101−411	17:16:06	59:51:00	···	DA	···	···	APO	06/01	600	0.18	355	9	72
G154−B5A/B	17:43:04	-13:17:18	11.92	dM3	14.41	DA	APO	09/00	300	0.09	25	32	33
LP44−310/311	18:28:00	69:58:00	18.46	DA	18.18	dM5	APO	04/01	3000	0.08	355	44	96
LP141−12/13	18:56:30	53:27:00	14.4	dM5	15.2	dM5	APO	04/01	500	0.23	103	170	1
LP141−14	18:56:30	53:27:00	18.5	DC	···	···	···	···	···	0.23	103	170	1
LP230−20/21	18:59:30	42:56:00	17.71	DC	18.12	dM4.5e	APO	09/00	1600	0.26	201	51	15
G142−B2A/B	19:11:20	13:31:18	14.07	DA	12.74	dM3	APO	09/00	300	0.10	180	155	19
L923−21/22	19:17:54	-07:45:00	12.31	DBZ5	12.14	dM5	APO	04/01	300	0.20	198	308	27
LP45−217/216	19:23:18	71:31:00	17.32	DA	16.33	dM5	APO	04/01	2100	0.16	8	262	3

TABLE 1 — *Continued*

Identifier (Sp.1/Sp.2) (1)	R.A. (B1950) (2)	Decl. (B1950) (3)	$V1$ (4)	Sp.1[a] (5)	$V2$ (6)	Sp.2[a] (7)	Site (8)	U.T. (mm/yy) (9)	Exp. (sec) (10)	μ ($''$/yr) (11)	Θ_μ (deg) (12)	Pos. (deg) (13)	Sep. ($''$) (14)
L852−36/37	19:32:54	-13:36:00	13.60	dM5	16.05	DA5	APO	04/01	500	0.14	189	205	28
LP813−18/17	19:43:11	-17:26:00	14.64	dM5	18.18	DC	APO	04/01	500	0.24	174	261	205
G24−10/9	20:11:32	06:32:30	13.27	dM5	15.78	DQ7	APO	04/01	500	0.70	206	331	100
LP575−17/18	20:27:36	06:45:00	17.51	DA	18.71	dM4.5e	APO	04-10/01	3000	0.22	32	29	77
LP575−16/15	20:27:36	07:20:00	16.14	DC5	17.18	dM4	APO	04/01	1800	0.26	135	313	39
LP46−147/148	20:41:00	73:08:00	18.77	DA	19.41	sdM0	APO	10/01	2400	0.07	90	227	19
LP696−4/5	20:44:42	-04:18:00	17.14	DA5	16.46	dM0	APO	06/01	2400	0.20	199	10	17
LP516−13/12	20:51:18	09:30:00	16.12	DA	17.02	dM5	APO	07/01	1800	0.13	0.0	318	10
Ross 193/VB11	20:54:06	-05:03:00	11.95	dM4e	16.71	DC9	APO	09/00	180	0.82	105	314	14
G212−B1A/B	21:07:59	42:44:48	15.62	DC5	15.65	dM	APO	09/00	1000	0.20	98	310	22
LP26−184/183	21:17:12	76:30:00	13.00	dM1	16.47	DA	APO	09/00,06/01	300	0.08	50	314	173
LP698−5/4	21:30:48	-06:24:00	16.42	dM2	18.52	DC	APO	09/00	1000	0.33	205	205	15
LP187−6/7	21:33:27	46:20:18	16.03	dM4.5e	17.97	DC	APO	09/00	900	0.46	200	64	3
LP398−18/19	21:38:30	21:27:00	16.98	DA	17.90	dM5e	APO	09/00	1800	0.12	195	100	81
LP458−49/48	21:48:06	19:39:00	17.94	DA	18.91	dM0	···	···	···	0.11	102	311	141
CD−51°13128/L283−7	21:54:24	-51:14:00	10.52	dM0e	14.77	DQ7	···	···	···	0.40	190	251	28
L427−60/61	21:54:48	-43:42:00	14.64	DB3	14.55	dMe	···	···	···	0.22	144	331	9
LP699−29/30	22:01:48	-03:46:00	15.95	dM5	18.26	DC9	APO	09/00	800	0.24	90	186	11
LP343−35/34	22:13:00	31:43:00	14.64	dM5	17.00	DA	APO	09/00	600	0.13	188	302	127
LP188−1/2	22:24:11	48:21:42	17.3	dM5	18.0	DAZ	APO	12/00,07/01	1500	0.59	41	86	2
L573−108/109	22:24:36	-34:27:00	14.44	DB3	12.99	dM0	···	···	···	0.21	94	15	9
LP400−22/21	22:34:06	22:16:48	17.22	DA	17.17	dM4.5e	APO	09-12/00,07/01	2400	0.20	74	288	338
LP761−113/114	22:49:20	-10:32:00	13.50	sdM3	17.39	DA	APO	09/00	300	0.19	157	332	7
LP2−696/697	22:53:12	81:14:00	11.77	dM0	17.39	DC	APO	09/00	180	0.23	63	134	8
LP581−36/35	22:53:24	05:30:00	11.24	dM2	16.19	DA	APO	06/01	180	0.45	127	286	17
LP345−26/27	22:56:18	31:19:00	13.96	dM	16.75	DA	APO	09/00	400	0.15	70	166	95
LP401−50/49	23:05:48	23:58:00	18.09	DC	18.14	dM4.5e	APO	09/00,10/01	2400	0.24	108	184	192
LP933−66/65	23:09:34	-27:37:36	15.47	dM5	17.08	DA	APO	09/00	900	0.21	98	215	66
LP522−34/35	23:18:00	12:42:00	16.27	DA	16.96	dM5e	APO	09/00,06/01	1000	0.18	72	50	35
LP762−53/54	23:18:32	-13:44:00	16.99	dM6e	18.79	DC	APO	09/00	1000	0.20	150	85	90
LP582−42/43	23:19:30	09:30:00	16.24	dM5	18.69	DC	APO	09/00	800	0.19	225	95	7
G275−B16A/B	23:23:30	-24:10:54	15.81	DA	15.73	dM0	APO	06-07/01	1800	0.05	200	202	12
LP77−37A/B	23:34:18	64:37:18	16.47	dM5	20.13	DA	APO	09/00	1200	0.21	114	300	5
LP463−27/26	23:36:24	20:45:00	14.24	dM5e	18.08	DC	APO	09/00,06/01	600	0.33	58	108	10
LP191−9/8	23:41:21	47:09:00	15.32	dM5	18.22	DC	APO	09/00	800	0.31	94	357	13
LP347−4/5	23:41:24	32:16:12	12.93	DA4	11.70	dM5	APO	09/00	300	0.24	256	9	175
G273−B15A/B	23:41:45	-16:27:30	14.29	dM2	15.97	DA	APO	09/00	800	0.14	210	5	5
LP935−14/15	23:44:36	-26:39:54	11.29	dM	16.59	DB	APO	06/01	90	0.36	255	141	14
LP2−246/247	23:48:00	84:31:00	18.90	DC	19.18	dM0	APO	12/00,07/01	3600	0.04	102	87	4
L577−71/72	23:51:31	-33:32:48	14.42	DA5	13.56	dM5	CTIO	01/02	400	0.50	217	0	7
LP524−35/34	23:54:12	05:23:00	12.45	dM1	18.31	DC	APO	09/00	120	0.21	69	210	148
LP348−19/20	23:58:54	27:03:00	17.34	DA	16.69	dM5	APO	09/00	1000	0.11	106	122	10

NOTE. — Single-precision V magnitude values are $m_{\rm pg}$ magnitudes from Luyten's original survey, all others are V magnitudes from Smith (1997).

[a] Spectral types for the WD and dM stars were determined from low-resolution (∼7-15 Å) spectra (Oswalt, Hintzen, & Luyten 1988; Oswalt et al. 1991, 1993). Improved dM spectral types are given in Table 3. We have made no attempt to improve upon the WD spectral types in this study.

TABLE 2
Journal of the Observations.

U.T. (yr) (1)	(mo) (2)	(day) (3)	Site (4)	Seeing (arcsec) (5)	Notes (6)
2000	Sep	04	APO	∼1.0	gibbous moon, clear
2000	Sep	05	APO	1.0	gibbous moon, clear
2000	Sep	06	APO	1.0	full moon, clear
2000	Sep	07	APO	0.8	partly cloudy
2000	Oct	03	APO	0.8	partly cloudy
2000	Dec	06	APO	∼1.0	clear
2001	Jan	24	APO	∼3.2	high humidity, variable seeing
2001	Jan	25	APO	2.7	high cirrus and humidity
2001	Jan	26	APO	1.2	clear
2001	Feb	04	APO	0.9	mostly cloudy
2001	Feb	12	APO	0.9	thick high cirrus
2001	Mar	01	APO	+2.0	A-half: closed - hit humidity limits
2001	Apr	01	APO	∼1.6	clouds, thick in west
2001	Apr	17	APO	1.8	B-half: closed - hit humidity/wind/dust limits
2001	Apr	26	APO	1.4	humidity near limits, partly cloudy
2001	Jun	19	APO	∼1.5	1^{st} half of A-half: closed - hit dust limits
2001	Jul	11	APO	1.4	1^{st} half of A-half: closed - hit dust limits and heavy clouds
2001	Sep	22	APO	···	1^{st} half of B-half: closed - hit wind limits and heavy clouds
2001	Oct	05	APO	∼1.5	thick high cirrus
2001	Oct	14	APO	1.9	clear
2001	Oct	15	APO	0.9	clear
2002	Jan	30	CTIO	∼1.4	gibbous moon, clear
2002	Jan	31	CTIO	∼1.0	gibbous moon, clear
2002	Feb	01	CTIO	∼1.2	gibbous moon, scattered high cirrus

TABLE 3
Equivalent Widths and BandHead Flux Ratios.

Identifier (dM) (1)	R.A. (B1950) (2)	Decl. (B1950) (3)	EW Hα (6563Å) (4)	$\sigma_{H\alpha}$ (+ Å) (5)	$\sigma_{H\alpha}$ (− Å) (6)	CaH1 (6385Å) (7)	CaH2 (6830Å) (8)	CaH3 (6975Å) (9)	TiO1 (6720Å) (10)	TiO2 (7059Å) (11)	TiO3 (7094Å) (12)	TiO4 (7132Å) (13)	TiO5 (7050Å) (14)	Sp.[a] (dM) (15)	Ref. (16)
LP349−14	00:22:06	27:24:00	-0.29	0.02	0.02	0.85	0.59	0.81	0.88	0.81	0.86	0.81	0.66	M1.0	3
G158−77	00:23:28	-10:53:30	-0.39	0.02	0.00	0.91	0.83	0.92	0.93	0.91	0.93	0.87	0.79	K7.5	3
G171−B10B	00:23:53	38:52:24	-0.10	0.05	0.00	0.84	0.43	0.73	0.80	0.58	0.71	0.64	0.39	M4.0	3
L170−14A	00:27:30	-54:58:00	3.33	0.02	0.26	0.86	0.44	0.71	0.81	0.48	0.67	0.61	0.34	M4.5	1
G218−7	00:38:30	55:33:42	-0.10	0.01	0.03	0.82	0.44	0.72	0.76	0.60	0.67	0.60	0.39	M4.0	3
Wolf 53	01:02:51	61:04:18	-0.03	0.00	0.02	0.76	0.49	0.73	0.78	0.69	0.75	0.69	0.47	M3.0	3
LP587−54	01:20:42	-02:24:48	-0.31	0.01	0.01	0.87	0.58	0.80	0.84	0.76	0.80	0.75	0.57	M2.0	3
G34−48	01:42:31	23:02:48	-0.19	0.00	0.01	0.86	0.65	0.82	0.88	0.82	0.85	0.81	0.67	M0.5	3
LP352−31	01:45:06	21:32:00	-0.17	0.02	0.02	0.84	0.50	0.76	0.82	0.69	0.73	0.67	0.48	M3.0	3
G244−37	01:48:12	64:11:24	-0.21	0.04	0.00	0.84	0.56	0.78	0.84	0.72	0.78	0.72	0.53	M2.5	3
G71−B5A	01:50:31	08:56:42	-0.27	0.03	0.02	0.87	0.56	0.79	0.85	0.72	0.80	0.74	0.57	M2.0	3
G272−B2B	01:58:32	-16:00:36	-0.05	0.04	0.01	0.80	0.48	0.70	0.77	0.69	0.72	0.72	0.46	M3.0	3
LP885−23	02:04:51	-30:38:30	-0.07	0.00	0.00	0.82	0.51	0.74	0.82	0.67	0.73	0.69	0.50	M2.5	3
LP590−142	02:25:52	00:24:30	-0.19	0.05	0.03	0.85	0.43	0.71	0.81	0.59	0.67	0.64	0.39	M4.0	3
LP355−11	02:57:42	24:42:00	-0.05	0.02	0.03	0.81	0.44	0.73	0.79	0.60	0.68	0.65	0.40	M3.5	3
LP472−38	03:17:18	11:24:00	-0.12	0.04	0.01	0.78	0.60	0.78	0.86	0.82	0.85	0.80	0.64	M1.0	3
LP31−140	03:24:30	73:15:00	0.20	0.06	0.00	0.82	0.41	0.70	0.77	0.54	0.64	0.60	0.33	M4.5	1
LP356−87	03:25:00	26:21:00	-0.10	0.01	0.00	0.83	0.55	0.79	0.82	0.74	0.79	0.76	0.54	M2.0	3
LP773−12	03:31:48	-16:05:00	0.11	0.01	0.00	0.82	0.48	0.73	0.80	0.69	0.72	0.69	0.47	M3.0	2
LP31−276	03:54:36	70:47:00	-0.21	0.02	0.00	0.87	0.65	0.83	0.87	0.85	0.86	0.85	0.69	M0.5	3
LP889−21	03:58:06	-32:06:00	-0.14	0.01	0.01	0.81	0.45	0.75	0.72	0.62	0.69	0.61	0.40	M3.5	3
LP415−1	04:17:12	19:47:00	-0.02	0.03	0.04	0.81	0.44	0.71	0.78	0.62	0.70	0.67	0.45	M3.0	3
LP775−52	04:19:26	-16:07:06	-0.24	0.00	0.00	0.85	0.64	0.82	0.85	0.85	0.86	0.83	0.68	M0.5	3
G175−34A	04:26:50	58:53:18	0.07	0.04	0.01	0.85	0.46	0.73	0.80	0.58	0.67	0.62	0.36	M4.0	2
HZ 9B	04:29:24	17:38:00	6.97	0.05	0.03	0.86	0.55	0.73	0.87	0.64	0.76	0.77	0.50	M2.5	1
LP891−13	04:43:18	-27:32:00	3.08	0.04	0.74	0.83	0.45	0.67	0.82	0.54	0.77	0.66	0.38	M4.0	1
G86−B1A	05:18:26	33:19:12	0.02	0.03	0.01	0.80	0.52	0.76	0.81	0.71	0.78	0.71	0.55	M2.0	2
LP779−20	06:04:18	-19:50:00	0.30	0.01	0.10	0.74	0.35	0.64	0.58	0.58	0.60	0.55	0.35	M4.5	2
LP600−43	06:28:08	-02:03:42	0.06	0.01	0.02	0.81	0.44	0.71	0.79	0.65	0.66	0.62	0.43	M3.5	2
LP205−28	06:41:50	43:48:36	0.26	0.04	0.01	0.92	0.45	0.77	0.76	0.65	0.66	0.65	0.43	M3.5	1
G87−28	07:06:52	37:45:24	-0.08	0.05	0.03	0.78	0.41	0.69	0.76	0.56	0.64	0.59	0.35	M4.5	3
LP422−7	07:09:18	19:24:00	-0.01	0.01	0.00	0.77	0.44	0.70	0.78	0.69	0.75	0.67	0.45	M3.0	3
LP207−8	07:26:06	39:17:00	-0.10	0.01	0.02	0.84	0.51	0.74	0.84	0.71	0.86	0.67	0.51	M2.5	3
G107−69	07:27:02	48:19:06	-0.26	0.05	0.04	0.81	0.41	0.70	0.76	0.56	0.65	0.58	0.36	M4.0	3
LP783−2	07:38:02	-17:17:24	-0.01	0.05	0.04	0.79	0.23	0.57	0.63	0.30	0.45	0.39	0.14	M6.5	3
LP366−2	07:41:37	24:50:24	-0.07	0.00	0.01	0.83	0.56	0.82	0.81	0.76	0.80	0.77	0.57	M2.0	3
LP208−33	08:04:18	44:40:00	-0.23	0.03	0.03	0.81	0.47	0.72	0.81	0.65	0.74	0.65	0.46	M3.0	3
LP664−16	08:06:30	-04:23:00	-0.15	0.02	0.00	0.86	0.61	0.82	0.83	0.80	0.83	0.80	0.63	M1.0	3
LP163−120	08:07:24	48:25:00	-0.16	0.04	0.04	0.86	0.52	0.77	0.82	0.69	0.78	0.67	0.50	M2.5	3
G111−72	08:16:47	38:44:18	-0.22	0.03	0.00	0.85	0.63	0.84	0.85	0.80	0.82	0.78	0.62	M1.5	3
L186−120	08:20:42	-58:32:00	-0.39	0.01	0.04	0.89	0.56	0.79	0.91	0.78	0.95	0.78	0.51	M2.5	3
LP164−51[b]	08:42:48	49:37:00	1.22	0.02	0.18	0.56	0.38	0.54	0.74	0.79	0.81	0.69	0.60	1.5	1
LP844−25	08:51:42	-24:36:00	0.66	0.03	0.02	0.62	0.21	0.47	0.65	0.41	0.48	0.42	0.22	M6.0	2
LP90−71	08:55:40	60:28:18	0.01	0.02	0.01	0.82	0.44	0.72	0.75	0.61	0.66	0.64	0.38	M4.0	2
LP845−9	08:58:42	-22:02:00	-0.24	0.03	0.00	0.83	0.61	0.82	0.83	0.83	0.85	0.80	0.67	M0.5	3
LP60−177	08:59:30	68:17:00	-0.15	0.00	0.00	0.88	0.72	0.86	0.90	0.90	0.92	0.92	0.82	K7.0	3
LP313−13	09:04:30	27:49:00	2.98	0.06	0.01	0.79	0.40	0.68	0.73	0.51	0.60	0.61	0.34	M4.5	1
LP313−15	09:06:18	29:42:00	-0.12	0.01	0.01	0.82	0.58	0.80	0.81	0.80	0.83	0.77	0.59	M1.5	3
LP60−237	09:11:24	65:09:00	-0.21	0.00	0.01	0.91	0.70	0.86	0.85	0.85	0.87	0.87	0.72	M0.0	3
LP487−26	09:16:00	11:11:00	0.04	0.00	0.04	0.84	0.38	0.70	0.71	0.52	0.62	0.53	0.31	M4.5	1
LP787−25	09:18:30	-17:16:00	0.16	0.00	0.08	1.06	0.56	0.87	1.08	1.19	1.15	1.19	0.72	M0.0	2
G117−B15B	09:21:13	35:29:48	2.64	0.00	0.01	0.78	0.41	0.67	0.75	0.60	0.67	0.65	0.39	M4.0	1

TABLE 3 — *Continued*

Identifier (dM) (1)	R.A. (B1950) (2)	Decl. (B1950) (3)	EW Hα (6563Å) (4)	$\sigma_{H\alpha}$ (+ Å) (5)	$\sigma_{H\alpha}$ (− Å) (6)	CaH1 (6385Å) (7)	CaH2 (6830Å) (8)	CaH3 (6975Å) (9)	TiO1 (6720Å) (10)	TiO2 (7059Å) (11)	TiO3 (7094Å) (12)	TiO4 (7132Å) (13)	TiO5 (7050Å) (14)	Sp.[a] (dM) (15)	Ref. (16)
G161−37	09:26:51	-03:57:00	-0.11	0.00	0.02	0.79	0.46	0.71	0.78	0.68	0.72	0.66	0.46	M3.0	3
LP488−20	09:37:42	09:21:00	0.00	0.02	0.01	0.77	0.38	0.66	0.71	0.62	0.68	0.59	0.35	M4.5	3
LP370−40	09:41:00	22:34:00	0.07	0.01	0.01	0.79	0.42	0.70	0.69	0.63	0.67	0.66	0.40	M3.5	1
G117−B11A	09:43:23	33:05:18	-0.25	0.02	0.02	0.80	0.45	0.71	0.79	0.66	0.74	0.65	0.45	M3.0	3
LP62−34A	10:04:36	66:34:00	-0.55	0.01	0.01	0.98	0.89	0.93	0.97	0.94	0.97	0.93	0.89	K6.5	3
LP847−41	10:10:18	-23:58:00	-0.28	0.00	0.05	0.92	0.66	0.82	0.92	0.81	0.96	0.80	0.58	M1.5	3
CD-18:3019	10:43:30	-18:50:00	-0.22	0.00	0.00	0.86	0.66	0.85	0.87	0.87	0.88	0.85	0.70	M0.5	3
LP317−25	10:54:24	30:30:00	-0.16	0.02	0.02	0.88	0.65	0.82	0.89	0.81	0.86	0.81	0.68	M0.5	3
LP214−39	11:05:12	41:16:00	-0.45	0.01	0.01	0.95	0.83	0.92	0.95	0.93	0.97	0.93	0.86	K6.5	3
LP672−2	11:05:30	-04:53:00	-0.10	0.01	0.01	0.85	0.48	0.75	0.80	0.70	0.74	0.70	0.47	M3.0	3
LP373−85	11:08:48	25:30:00	0.29	0.01	0.01	0.81	0.42	0.70	0.78	0.62	0.70	0.62	0.38	M4.0	1
LP792−6	11:11:30	-18:47:00	-0.03	0.03	0.06	0.86	0.43	0.73	0.78	0.55	0.67	0.59	0.37	M4.0	3
LP552−48	11:20:54	07:18:00	-0.46	0.01	0.01	0.96	0.84	0.93	0.92	0.92	0.94	0.90	0.79	K7/M0	3
LP906−23	11:20:54	-32:07:00	-0.32	0.01	0.02	0.92	0.60	0.80	0.88	0.70	0.84	0.73	0.49	M2.5	3
LP906−34	11:32:54	-29:53:00	-0.06	0.05	0.00	1.00	0.66	0.89	1.05	1.22	1.11	1.11	0.86	K6.5	3
G148−6	11:43:21	32:06:12	0.10	0.01	0.04	0.81	0.44	0.70	0.79	0.60	0.70	0.63	0.43	M3.5	1
LP375−50	11:47:46	25:35:18	9.60	0.01	0.00	0.78	0.45	0.68	0.80	0.58	0.70	0.70	0.41	M3.5	1
LP493−61	11:48:48	13:11:00	-0.21	0.00	0.01	0.86	0.65	0.85	0.84	0.83	0.84	0.82	0.62	M1.5	3
LP129−586	11:48:48	54:28:00	0.07	0.02	0.01	0.79	0.45	0.70	0.78	0.70	0.74	0.72	0.48	M3.0	2
LP216−75	12:11:06	39:18:00	-0.18	0.00	0.01	0.90	0.76	0.88	0.90	0.92	0.94	0.93	0.84	K7.0	3
LP554−64	12:14:18	03:14:00	-0.27	0.01	0.04	0.84	0.46	0.73	0.80	0.60	0.71	0.63	0.43	M3.5	3
LP435−59	12:20:24	19:06:00	-0.11	0.04	0.06	0.82	0.47	0.73	0.77	0.62	0.73	0.65	0.44	M3.5	3
LP795−14	12:22:48	-16:50:00	0.18	0.02	0.03	0.82	0.51	0.78	0.78	0.74	0.72	0.71	0.49	M2.5	2
LP495−176	12:30:36	12:16:00	-0.04	0.05	0.05	0.89	0.48	0.76	0.80	0.62	0.72	0.65	0.46	M3.0	3
LP321−205	12:30:42	26:22:00	-0.01	0.04	0.06	0.85	0.42	0.73	0.63	0.59	0.62	0.63	0.39	M4.0	3
G61−16	12:44:44	14:58:24	-0.30	0.01	0.02	0.84	0.66	0.84	0.88	0.87	0.91	0.86	0.76	K7/M0	3
LP497−29	13:11:30	11:14:00	-0.13	0.07	0.03	0.83	0.36	0.69	0.73	0.53	0.65	0.59	0.34	M4.5	3
HZ 43B	13:14:00	29:22:00	1.42	0.00	0.03	0.93	0.70	0.81	0.90	0.70	0.83	0.81	0.64	M1.0	1
LP617−34	13:17:42	-02:08:00	6.55	0.08	0.06	0.81	0.38	0.69	0.78	0.51	0.63	0.62	0.34	M4.5	1
G14−57	13:27:40	-08:18:48	-0.17	0.04	0.03	0.84	0.39	0.71	0.76	0.53	0.64	0.58	0.35	M4.5	3
LP798−14	13:34:18	-16:04:00	2.29	0.05	0.03	0.84	0.53	0.76	0.87	0.73	0.81	0.76	0.61	M1.5	1
LP738−42	13:34:48	-11:48:00	-0.35	0.02	0.04	0.86	0.48	0.76	0.80	0.60	0.71	0.64	0.42	M3.5	3
LP498−25	13:36:45	12:23:48	-0.28	0.00	0.05	0.86	0.53	0.78	0.83	0.68	0.77	0.69	0.51	M2.5	3
LP219−78	13:48:18	41:48:00	0.22	0.08	0.03	0.86	0.36	0.66	0.79	0.55	0.66	0.58	0.33	M4.5	1
LP856−54	13:48:30	-27:19:00	-0.27	0.03	0.01	0.85	0.59	0.81	0.86	0.79	0.83	0.79	0.63	M1.0	3
LP439−180	14:00:42	16:04:00	-0.12	0.03	0.02	0.76	0.38	0.69	0.77	0.55	0.65	0.61	0.33	M4.5	3
LP133−373[c]	14:02:24	50:36:00	7.70	0.08	0.07	0.80	0.41	0.66	0.77	0.55	0.67	0.64	0.37	M4.0	1
LP799−74	14:09:36	-18:29:00	0.27	0.07	0.00	0.75	0.35	0.64	0.76	0.54	0.66	0.58	0.36	M4.0	1
LP66−587	14:16:06	63:18:00	-0.10	0.03	0.00	0.80	0.56	0.78	0.84	0.78	0.81	0.77	0.63	M1.0	3
G200−40	14:25:59	54:01:00	-0.27	0.02	0.01	0.92	0.80	0.90	0.93	0.91	0.93	0.90	0.81	K7.0	3
LP135−155	15:10:34	56:36:12	0.03	0.02	0.02	0.76	0.45	0.73	0.79	0.66	0.71	0.64	0.42	M3.5	2
LP223−14	15:25:30	43:23:30	-0.14	0.03	0.03	0.78	0.53	0.78	0.81	0.75	0.76	0.69	0.57	M2.0	3
LP176−59	15:33:12	46:59:00	-0.41	0.09	0.01	0.79	0.28	0.59	0.67	0.40	0.53	0.46	0.23	M5.5	3
LP743−25	15:39:12	-13:47:00	-0.05	0.08	0.01	0.72	0.35	0.65	0.71	0.53	0.65	0.61	0.37	M4.0	3
LP916−26	15:42:18	-27:30:00	-0.17	0.05	0.02	0.83	0.39	0.69	0.79	0.56	0.68	0.62	0.38	M4.0	3
G152−B4A	15:55:22	-08:59:30	-0.05	0.03	0.02	0.81	0.52	0.77	0.81	0.73	0.75	0.71	0.50	M2.5	3
LP101−15	16:33:30	57:15:00	1.91	0.05	0.15	0.81	0.39	0.66	0.79	0.51	0.69	0.57	0.34	M4.5	1
LP505−43	16:35:00	11:16:00	-0.18	0.05	0.03	0.82	0.51	0.77	0.87	0.74	0.83	0.73	0.60	M1.5	3
LP686−33	16:56:12	-06:11:00	0.19	0.02	0.01	0.74	0.42	0.67	0.77	0.64	0.71	0.64	0.43	M3.5	2
LP387−37	17:03:54	26:10:00	-0.23	0.02	0.02	0.85	0.61	0.82	0.86	0.76	0.82	0.76	0.61	M1.5	3
Wolf 672B	17:16:05	02:00:12	-0.19	0.07	0.02	0.85	0.40	0.71	0.80	0.56	0.68	0.61	0.40	M3.5	3
G154−B5A	17:43:04	-13:17:18	-0.11	0.02	0.03	0.90	0.68	0.85	0.94	0.87	0.94	0.88	0.80	K7/M0	3
LP44−311	18:28:00	69:58:00	-0.33	0.02	0.04	0.83	0.45	0.72	0.85	0.69	0.73	0.63	0.45	M3.0	3
LP230−21	18:59:30	42:56:00	0.04	0.00	0.00	0.79	0.32	0.65	0.75	0.44	0.59	0.50	0.25	M5.5	2

TABLE 3 — *Continued*

Identifier (dM) (1)	R.A. (B1950) (2)	Decl. (B1950) (3)	EW Hα (6563Å) (4)	$\sigma_{H\alpha}$ (+ Å) (5)	$\sigma_{H\alpha}$ (− Å) (6)	CaH1 (6385Å) (7)	CaH2 (6830Å) (8)	CaH3 (6975Å) (9)	TiO1 (6720Å) (10)	TiO2 (7059Å) (11)	TiO3 (7094Å) (12)	TiO4 (7132Å) (13)	TiO5 (7050Å) (14)	Sp.[a] (dM) (15)	Ref. (16)
G142−B2B	19:11:20	13:31:18	-0.19	0.04	0.01	0.82	0.51	0.76	0.84	0.75	0.80	0.75	0.58	M1.5	3
L923−22	19:17:54	-07:45:00	-0.14	0.02	0.04	0.77	0.44	0.71	0.80	0.67	0.73	0.69	0.50	M2.5	3
LP45−216	19:23:18	71:31:00	-0.17	0.01	0.01	0.77	0.47	0.71	0.80	0.70	0.75	0.70	0.49	M2.5	3
L852−36	19:32:54	-13:36:00	-0.41	0.02	0.04	0.89	0.70	0.87	0.92	0.84	0.91	0.86	0.77	K7/M0	3
LP813−18	19:43:11	-17:26:00	-0.42	0.04	0.03	0.85	0.50	0.76	0.81	0.69	0.81	0.72	0.50	M2.5	3
G24−10	20:11:32	06:32:30	-0.12	0.03	0.03	0.83	0.43	0.74	0.79	0.59	0.69	0.64	0.42	M3.5	3
LP575−18	20:27:36	06:45:00	-0.23	0.18	0.13	0.76	0.28	0.54	0.69	0.40	0.61	0.53	0.24	M5.5	3
LP575−15	20:27:36	07:20:00	-0.33	0.02	0.04	0.79	0.32	0.65	0.80	0.50	0.60	0.57	0.32	M4.5	3
LP698−5	20:44:42	-04:18:00	-0.06	0.04	0.01	0.82	0.41	0.71	0.78	0.63	0.71	0.64	0.44	M3.5	3
Ross 193	20:54:06	-05:03:00	1.61	0.04	0.03	0.81	0.42	0.69	0.80	0.57	0.67	0.62	0.39	M4.0	1
G212−B1B	21:07:59	42:44:48	-0.01	0.02	0.03	0.79	0.46	0.71	0.77	0.69	0.72	0.66	0.44	M3.5	3
LP26−184	21:17:12	76:30:00	-0.37	0.03	0.01	0.99	0.83	0.92	0.92	0.94	0.97	0.96	0.90	K6.0	3
LP696−5	21:30:48	-06:24:00	-0.20	0.04	0.01	0.77	0.41	0.69	0.80	0.63	0.72	0.64	0.46	M3.0	3
LP187−6	21:33:27	46:20:18	-0.15	0.00	0.03	0.87	0.41	0.73	0.78	0.56	0.63	0.56	0.33	M4.5	3
LP398−19	21:38:30	21:27:00	-0.05	0.03	0.02	0.85	0.46	0.73	0.83	0.65	0.71	0.66	0.42	M3.5	3
LP699−29	22:01:48	-03:46:00	-0.29	0.06	0.01	0.79	0.50	0.73	0.76	0.69	0.77	0.70	0.52	M2.5	3
LP343−35	22:13:00	31:43:00	-0.16	0.01	0.01	0.85	0.51	0.76	0.81	0.67	0.75	0.70	0.47	M3.0	3
LP400−21	22:34:06	22:16:48	-0.14	0.03	0.02	0.78	0.41	0.67	0.77	0.59	0.67	0.62	0.38	M4.0	3
LP2−696	22:53:12	81:14:00	-0.35	0.01	0.03	0.90	0.81	0.91	0.91	0.85	0.90	0.84	0.73	M0.0	3
LP581−36	22:53:24	05:30:00	-0.35	0.04	0.02	0.87	0.58	0.82	0.87	0.81	0.83	0.81	0.65	M1.0	3
LP401−49	23:05:48	23:58:00	-0.17	0.07	0.04	0.79	0.36	0.68	0.77	0.46	0.60	0.55	0.30	M5.0	3
LP933−66	23:09:34	-27:37:36	-0.27	0.03	0.05	0.82	0.49	0.75	0.83	0.68	0.75	0.68	0.50	M2.5	3
LP522−35	23:18:00	12:42:00	-0.44	0.05	0.06	0.86	0.47	0.73	0.80	0.58	0.74	0.62	0.41	M3.5	3
LP762−53	23:18:32	-13:44:00	13.38	0.05	0.09	0.85	0.42	0.69	0.80	0.45	0.67	0.65	0.33	M4.5	1
LP582−42	23:19:30	09:30:00	-0.12	0.00	0.02	0.79	0.45	0.71	0.78	0.62	0.71	0.65	0.42	M3.5	3
LP77−37A	23:34:18	64:37:18	0.11	0.03	0.00	0.79	0.40	0.69	0.77	0.66	0.70	0.67	0.42	M3.5	2
LP463−27	23:36:24	20:45:00	4.83	0.19	0.06	0.78	0.38	0.64	0.78	0.55	0.69	0.65	0.39	M4.0	1
LP191−9	23:41:21	47:09:00	0.05	0.03	0.02	0.77	0.42	0.71	0.80	0.71	0.74	0.70	0.47	M3.0	2
LP347−5	23:41:24	32:16:12	-0.09	0.04	0.01	0.80	0.45	0.73	0.80	0.69	0.75	0.70	0.49	M2.5	3
G273−B15A	23:41:45	-16:27:30	-0.14	0.03	0.00	0.83	0.58	0.80	0.88	0.81	0.85	0.81	0.67	M0.5	3
LP935−14	23:44:36	-26:39:54	-0.47	0.03	0.01	0.97	0.75	0.89	0.96	0.89	0.94	0.91	0.82	K7.0	3
L577−72	23:51:31	-33:32:48	-0.40	0.01	0.01	0.87	0.64	0.79	0.88	0.73	0.82	0.76	0.60	M1.5	3
LP524−35	23:54:12	05:23:00	-0.39	0.01	0.00	0.92	0.87	0.91	0.89	0.90	0.92	0.89	0.80	K7/M0	3
LP348−20	23:58:54	27:03:00	-0.30	0.02	0.03	0.81	0.50	0.75	0.80	0.66	0.71	0.67	0.47	M3.0	3

REFERENCES. — (1) dMe Stars; (2) dM(e) Stars; (3) dM Stars.

[a] Improved dM spectral types based on TiO5 bandhead ratios.
[b] Stellar halo white dwarf candidate.
[c] M dwarf has close (eclipsing) companion.

TABLE 4
PARAMETERS FOR THE dME AND dM(E) STARS.

Identifier (dM) (1)	R.A. (B1950) (2)	Decl. (B1950) (3)	$V-I$ (4)	M_V (5)	Mass ($M_\odot$) (6)
		dMe Stars			
L170−14A	00:27:30	-54:58:00	3.30	13.51	0.18
LP31−140	03:24:30	73:15:00	3.09	13.01	0.21
HZ 9B	04:29:24	17:38:00	2.52	11.34	0.34
LP891−13	04:43:18	-27:32:00	2.86	13.00	0.21
LP205−28	06:41:50	43:48:36	2.59	11.55	0.32
LP313−13	09:04:30	27:49:00	3.07	12.94	0.21
LP487−26	09:16:00	11:11:00	3.23	13.35	0.19
G117−B15B	09:21:13	35:29:48	2.77	12.11	0.27
LP370−40	09:41:00	22:34:00	2.82	12.27	0.26
LP373−85	11:08:48	25:30:00	2.92	13.00	0.21
G148−6	11:43:21	32:06:12	2.67	11.80	0.30
LP375−50	11:47:46	25:35:18	2.71	11.93	0.29
HZ 43B	13:14:00	29:22:00	2.04	9.75	0.52
LP617−34	13:17:42	-02:08:00	2.94	13.00	0.21
LP798−14	13:34:18	-16:04:00	2.18	10.22	0.46
LP219−78	13:48:18	41:48:00	2.07	9.83	0.51
LP133−373	14:02:24	50:36:00	2.87	13.00	0.21
LP799−74	14:09:36	-18:29:00	3.08	12.97	0.21
LP101−15	16:33:30	57:15:00	2.88	13.00	0.21
Ross 193	20:54:06	-05:03:00	2.72	11.97	0.28
LP762−53	23:18:32	-13:44:00	3.15	13.15	0.20
LP463−27	23:36:24	20:45:00	2.76	12.07	0.28
		dM(e) Stars			
LP773−12	03:31:48	-16:05:00	2.55	11.45	0.33
G175−34A	04:26:50	58:53:18	2.86	13.00	0.21
G86−B1A	05:18:26	33:19:12	2.37	10.87	0.39
LP779−20	06:04:18	-19:50:00	3.17	13.21	0.20
LP600−43	06:28:08	-02:03:42	3.15	13.15	0.20
LP844−25	08:51:42	-24:36:00	3.76	14.35	0.15
LP90−71	08:55:40	60:28:18	2.77	12.12	0.27
LP787−25	09:18:30	-17:16:00	3.24	13.36	0.19
LP129−586	11:48:48	54:28:00	2.53	11.36	0.55
LP795−14	12:22:48	-16:50:00	2.39	10.92	0.38
LP135−155	15:10:34	56:36:12	2.59	11.55	0.32
LP686−33	16:56:12	-06:11:00	2.74	12.02	0.28
LP230−21	18:59:30	42:56:00	3.71	14.27	0.15
LP77−37A	23:34:18	64:37:18	2.78	12.14	0.27
LP191−9	23:41:21	47:09:00	2.47	11.20	0.36

TABLE 5
Complete Space Motions for 161 M Dwarf Stars.

Identifier (dM) (1)	R.A. (B1950) (2)	Decl. (B1950) (3)	μ ($''$/yr) (4)	Θ (deg) (5)	v_r (km/s) (6)	σ_{v_r} (km/s) (7)	U (km/s) (8)	σ_U (km/s) (9)	V (km/s) (10)	σ_V (km/s) (11)	W (km/s) (12)	σ_W (km/s) (13)	Sp.V. (km/s) (14)	$\sigma_{\rm Sp.V.}$ (km/s) (15)	Ref. (16)
LP349−14	00.3683	27.4000	0.12	90	48.6	3.5	37.2	0.9	7.4	1.9	-38.2	2.8	53.8	0.1	3
G158−77	00.3911	-10.8917	0.27	160	52.2	6.4	-27.6	0.9	-110.5	3.2	-93.5	5.5	147.3	0.0	3
G171−B10B	00.3981	38.8733	0.20	132	19.4	2.9	20.1	0.9	-22.5	1.8	-46.0	2.1	55.0	0.0	3
L170−14A	00.4583	-54.8917	0.36	240	16.2	14.8	-43.8	6.0	-16.4	9.9	-11.9	9.2	48.2	0.2	1
G218−8	00.6417	55.5589	0.32	103	20.5	8.5	21.2	3.5	-7.5	5.7	-15.9	5.2	27.5	0.2	3
LP825−712	00.6767	-22.0333	0.50	83	11.9	30.0	53.1	7.2	-39.8	16.0	-20.3	24.3	69.4	0.3	4
LP242−11	00.8750	32.5333	0.50	242	22.8	33.6	-159.5	10.6	58.1	19.3	-96.8	25.4	195.4	0.1	2,4
LP1−169	01.0167	86.6667	0.13	73	23.7	5.1	11.6	2.5	-1.7	3.8	6.5	2.4	13.4	0.3	2,4
Wolf 53	01.0475	61.0717	0.48	137	23.9	25.7	76.0	11.3	-44.4	17.8	-92.7	14.7	127.9	0.1	3
LP587−54	01.3450	-02.4133	0.22	79	9.8	8.9	22.6	2.7	-23.4	4.4	-9.3	7.3	33.8	0.2	3
G34−48	01.7086	23.0467	0.32	112	32.9	7.4	58.5	3.0	-58.3	4.0	-34.8	5.5	89.6	0.1	3
LP352−31	01.7517	21.5333	0.20	80	15.3	7.3	54.6	3.0	-39.4	3.9	6.9	5.5	67.7	0.1	3
G244−37	01.8033	64.1900	0.29	129	14.3	7.6	14.3	3.6	-12.2	5.3	-15.2	4.1	24.2	0.2	3
G71−B5A	01.8419	08.9450	0.10	154	31.3	6.7	6.6	2.8	-26.0	3.3	-42.8	5.1	50.5	0.1	3
G272−B2B	01.9756	-16.0100	0.13	81	16.6	19.8	35.7	8.7	-36.6	10.1	-8.4	14.7	51.8	0.3	3
LP885−23	02.0808	-30.6417	0.25	124	16.9	14.1	2.1	6.5	-50.4	7.9	-13.7	9.7	52.2	0.2	3
LP245−18	02.2892	37.5633	0.35	102	5.8	8.6	74.2	4.2	-97.4	5.1	8.4	5.5	122.8	0.1	2,4
LP590−142	02.4311	00.4083	0.11	155	13.9	8.3	-8.6	4.3	-56.6	4.0	-31.3	5.9	65.3	0.1	3
LP355−11	02.9617	24.7000	0.18	124	-26.5	8.9	3.2	5.3	-100.9	4.7	4.5	5.4	101.0	0.1	3
LP472−38	03.2883	11.4000	0.18	192	9.7	6.6	-31.5	4.3	-50.9	3.2	-60.7	3.8	85.2	0.1	3,4
LP355−64	03.3250	26.9833	0.18	124	27.6	25.2	65.9	16.0	-135.1	13.5	-12.6	14.0	150.8	0.1	3,4
LP31−140	03.4083	73.8500	0.43	141	0.0	7.7	66.1	3.9	-73.5	5.6	-33.7	3.6	104.5	0.1	1
LP356−87	03.4167	26.3500	0.18	120	-10.8	6.7	-4.0	4.3	-50.5	3.6	2.3	3.6	50.7	0.1	3
LP888−63	03.4458	-27.3100	0.83	63	17.0	25.4	14.3	16.5	-24.8	13.7	-9.7	13.7	30.2	0.6	3,4
LP773−12	03.5300	-16.0833	0.32	80	14.0	9.3	44.9	6.4	-57.8	4.6	30.6	5.0	79.3	0.1	2
LP31−276	03.9100	70.7833	0.17	74	5.1	7.4	4.1	3.8	-31.2	5.3	29.1	3.4	42.9	0.1	3
LP889−21	03.9683	-32.1000	0.21	117	13.3	13.6	-5.6	9.4	-71.0	7.6	17.3	6.4	73.3	0.1	3
LP415−1	04.2867	19.7833	0.17	216	-23.1	7.0	-52.7	5.3	-30.0	3.5	-59.8	2.9	85.2	0.1	3
LP775−52	04.3239	-16.1183	0.35	112	37.8	5.9	17.4	4.6	-79.4	2.9	2.6	2.4	81.3	0.1	3
G175−34A	04.4489	58.8667	2.37	146	2.1	9.8	17.9	5.7	-49.4	6.7	-14.2	4.3	54.5	0.1	2
HZ 9B	04.4900	17.6333	0.12	110	-10.4	9.8	-17.8	7.7	-16.7	4.8	-0.9	3.8	24.4	0.3	1
LP358−52B	04.5483	26.9333	0.11	108	23.4	6.0	14.5	4.5	-12.5	3.2	-10.4	2.3	21.8	0.2	3,4
LP891−13	04.7217	-27.5333	0.24	246	22.2	41.2	-15.9	31.5	-13.1	21.9	-47.4	15.1	51.7	0.6	1
G86−B1A	05.3072	33.3200	0.18	113	52.4	9.3	47.6	7.1	-40.2	5.2	12.8	3.0	63.6	0.1	2
LP159−33	05.8664	46.8483	0.54	179	36.7	37.0	29.6	25.6	-13.0	23.1	-5.7	13.3	32.8	0.8	3
LP779−20	06.0717	-19.8333	0.23	108	24.8	10.8	-29.4	9.0	-103.1	5.3	69.1	2.6	127.5	0.1	2
LP600−43	06.4689	-02.0617	0.25	214	-14.9	7.9	-33.4	6.8	-17.0	3.6	-36.9	1.7	52.6	0.1	2
LP205−28	06.6972	43.8100	0.12	176	-11.8	8.4	9.4	5.9	-138.3	5.1	-49.2	3.1	147.1	0.0	1
G87−28	07.1144	37.7567	0.44	222	-4.6	10.2	4.4	7.4	-39.8	5.9	-57.8	3.8	70.4	0.1	3
LP422−7	07.1550	19.4000	0.10	147	-4.2	7.9	-26.9	6.3	-50.0	3.9	-2.1	2.6	56.8	0.1	3
LP5−74	07.4333	82.7333	0.18	76	14.4	7.8	-51.2	3.8	-13.4	5.8	76.7	3.6	93.2	0.1	···
LP207−8	07.4350	39.2833	0.12	186	44.3	9.6	38.8	6.7	-52.5	5.7	-5.0	3.9	65.5	0.1	3
G107−69	07.4506	48.3183	1.34	191	-0.9	10.6	17.2	6.9	-82.4	6.7	-36.4	4.5	91.7	0.1	3
LP783−2	07.6342	-17.2900	1.26	117	-10.0	13.5	-115.5	10.4	-72.9	6.6	72.5	5.5	154.7	0.1	3
LP366−2	07.6936	24.8400	0.10	260	-13.1	6.6	-2.3	4.9	-4.9	3.4	-53.1	2.8	53.3	0.1	3
LP208−33	08.0717	44.6667	0.10	200	3.9	8.6	2.9	5.4	-34.5	5.3	-15.8	4.0	38.1	0.2	3
LP664−16	08.1083	-04.3833	0.12	182	18.8	6.9	-9.0	5.1	-41.8	3.2	-14.5	3.3	45.1	0.1	3
LP163−120	08.1233	48.4167	0.14	79	17.9	9.5	-30.0	5.8	-9.1	6.0	57.4	4.5	65.4	0.1	3
G111−72	08.2797	38.7383	0.38	212	19.9	6.5	30.7	4.2	-65.2	3.8	-35.3	3.2	80.3	0.1	3
L186−120	08.3450	-58.5333	0.20	289	51.0	···	40.2	···	-56.4	···	-57.1	···	89.8	···	3
LP164−51[a]	08.7133	49.6167	0.31	159	24.0	12.3	-0.7	7.0	-136.6	7.9	48.7	6.3	145.0	0.1	1,4
LP844−25	08.8617	-24.6000	0.64	78	-0.1	15.9	-89.4	9.8	-6.9	8.4	137.1	9.3	163.8	0.1	2
LP60−359B	08.8733	63.0500	0.11	110	22.1	18.8	-0.5	9.8	-9.1	13.1	17.6	9.3	19.8	0.7	1

TABLE 5 — *Continued*

Identifier (dM) (1)	R.A. (B1950) (2)	Decl. (B1950) (3)	μ ($''$/yr) (4)	Θ (deg) (5)	v_r (km/s) (6)	σ_{v_r} (km/s) (7)	U (km/s) (8)	σ_U (km/s) (9)	V (km/s) (10)	σ_V (km/s) (11)	W (km/s) (12)	σ_W (km/s) (13)	Sp.V. (km/s) (14)	$\sigma_{\rm Sp.V.}$ (km/s) (15)	Ref. (16)
LP90−71	08.9278	60.4717	0.53	216	-0.8	8.1	68.2	4.2	-108.1	5.6	-46.3	4.1	135.9	0.0	2
LP845−9	08.9783	-22.0333	0.19	319	26.8	6.6	72.3	4.0	-8.8	3.4	-2.5	4.0	72.9	0.1	3
LP60−177	08.9917	68.2833	0.16	215	12.9	5.5	83.6	2.8	-96.2	3.9	-24.9	2.7	129.9	0.0	3
LP313−13	09.0750	27.8167	0.13	160	11.1	10.9	-20.4	6.4	-60.4	5.9	4.6	6.6	63.9	0.1	1
LP313−15	09.1050	29.7000	0.14	237	24.0	7.0	49.9	4.0	-61.5	3.9	-50.4	4.2	93.9	0.1	3
LP60−237	09.1900	65.1500	0.14	241	17.6	7.7	44.0	3.9	-30.0	5.4	-23.6	3.9	58.3	0.1	3
LP487−26	09.2667	11.1833	0.35	235	8.6	10.0	34.4	5.7	-69.9	4.9	-84.4	6.6	114.9	0.1	1
LP787−25	09.3083	-17.2667	0.20	323	-10.4	37.0	55.8	20.8	26.4	18.7	-6.9	24.3	62.1	0.4	3
G117−B15B	09.3536	35.4967	0.14	264	2.3	9.4	20.3	5.0	-17.6	5.5	-33.1	5.8	42.7	0.2	1
G161−37	09.4475	-03.9500	0.27	274	13.8	9.9	47.4	5.4	-21.8	4.7	-42.5	6.8	67.3	0.1	0
LP488−20	09.6283	09.3500	0.26	255	10.1	10.2	40.6	5.2	-38.5	5.0	-52.4	7.2	76.6	0.1	2
LP370−40	09.6833	22.5667	0.12	201	-21.8	8.0	-21.1	4.0	-71.6	4.2	-53.3	5.5	91.7	0.1	1
G117−B11A	09.7231	33.0883	0.14	133	10.9	9.4	-24.1	4.6	-33.3	5.4	15.6	6.2	44.0	0.2	3
LP62−34A	10.0767	66.5667	0.21	224	22.7	11.1	59.8	5.3	-65.9	7.9	0.5	5.8	88.9	0.1	3
LP847−41	10.1717	-23.9667	0.18	312	60.2	···	83.4	···	-52.6	···	23.3	···	101.3	7.0	3
CD−18°3019	10.7250	-18.8333	1.98	250	40.3	6.5	123.4	2.1	-134.4	3.4	-125.5	5.2	221.5	0.0	3
LP317−25	10.9067	30.5000	0.16	270	36.0	7.8	80.4	2.6	-42.6	4.4	-11.7	5.9	91.7	0.1	3
LP214−39	11.0867	41.2667	0.21	275	34.7	9.2	57.6	3.3	-24.1	5.7	0.8	6.5	62.4	0.1	3
LP672−2	11.0917	-04.8833	0.44	184	24.0	7.1	-23.7	1.6	-55.7	3.5	-10.7	6.0	61.5	0.1	3
LP373−85	11.1467	25.5833	0.24	266	13.5	11.1	60.3	3.1	-45.3	6.1	-24.0	8.8	79.2	0.1	1
LP792−6	11.1917	-18.7833	0.25	300	24.6	9.4	31.7	2.3	-32.7	4.9	9.5	7.7	46.5	0.1	3
LP552−48	11.3483	07.3000	0.20	110	39.5	8.7	-77.4	1.5	-25.6	4.3	42.1	7.4	91.8	0.1	3
LP906−23	11.3483	-32.1167	0.24	282	64.1	···	11.9	···	-77.8	···	16.7	···	80.4	···	3
LP906−34	11.5483	-29.8833	0.16	227	70.6	···	-6.5	···	-98.8	···	-10.9	···	99.7	···	3
LP493−16	11.5633	08.3167	0.25	245	25.6	17.4	24.0	2.4	-58.8	8.7	-4.5	14.9	63.6	0.2	3
G148−6	11.7225	32.1033	0.28	203	23.3	10.7	-4.5	2.9	-50.5	6.2	14.0	8.3	52.6	0.1	1
LP375−50	11.7961	25.5883	0.30	252	14.7	10.9	44.9	2.4	-64.1	6.0	-10.2	8.8	78.9	0.1	1
LP493−61	11.8133	13.1833	0.21	182	27.7	21.5	-44.2	2.9	-93.4	10.9	-2.9	18.3	103.3	0.2	3
LP129−586	11.8133	54.4667	0.25	264	6.0	6.1	94.9	2.4	-72.3	4.1	-24.1	3.8	121.7	0.0	2
LP673−42A	11.8453	-07.0933	0.54	198	28.9	17.4	-18.3	1.7	-57.7	8.7	-6.1	15.0	60.9	0.2	3
LP554−64	12.2383	03.2333	0.70	293	31.1	10.5	45.1	1.0	-33.2	5.2	23.2	9.1	60.6	0.1	3
LP320−644	12.2517	32.3667	0.26	234	15.1	7.3	12.1	2.0	-52.2	4.2	5.3	5.6	53.8	0.1	3,4
LP435−59	12.3400	19.1000	0.19	268	14.2	7.2	68.5	1.3	-62.2	3.8	-3.6	6.0	92.6	0.1	3
LP795−14	12.3800	-16.8333	0.12	211	46.0	8.9	-13.5	1.6	-118.4	4.6	-40.2	7.5	125.7	0.1	2
LP495−176	12.5100	12.2667	0.16	284	25.2	13.5	62.1	2.2	-41.4	6.8	16.8	11.4	76.5	0.1	3
LP321−205	12.5117	26.3667	0.15	263	-3.5	12.0	65.6	3.0	-70.0	6.6	-17.4	9.6	97.5	0.1	3
G61−16	12.7456	14.9733	0.43	298	20.2	5.2	134.7	1.1	-28.9	2.7	25.4	4.3	140.1	0.0	3
LP497−30	13.1917	11.2333	0.24	207	-22.5	6.2	-14.2	1.8	-97.8	3.1	-47.9	5.1	109.8	0.0	3
HZ 43B	13.2333	29.3667	0.16	240	44.4	14.4	160.7	4.9	-396.0	8.1	79.6	10.9	434.7	0.0	1,4
LP617−34	13.2950	-02.1333	0.19	159	7.3	8.5	-29.0	2.5	-25.8	4.2	-12.6	7.0	40.8	0.2	1
G14−57	13.4581	-08.3133	1.24	247	35.7	4.8	37.0	1.6	-118.0	2.4	11.4	3.9	124.2	0.0	3
LP798−14	13.5717	-16.0667	0.12	246	54.1	2.7	-21.2	1.0	-61.1	1.4	27.9	2.1	70.4	0.0	1
LP738−42	13.5800	-11.8000	0.19	199	35.1	9.3	-34.2	3.4	-81.1	4.7	-15.4	7.3	89.4	0.1	3,4
LP498−25	13.6125	12.3967	0.19	134	50.3	9.1	-63.7	3.4	-21.3	4.6	27.5	7.1	72.6	0.1	3
LP219−78	13.8050	41.8000	0.14	160	24.9	22.9	-217.6	10.1	-111.4	14.1	49.1	15.0	249.3	0.1	1
LP856−54	13.8083	-27.3167	0.24	199	49.9	4.3	-38.8	1.8	-71.0	2.4	-9.2	3.1	81.5	0.0	3
LP439−180	14.0117	16.0667	0.08	167	9.5	8.7	-32.1	3.9	-28.0	4.4	-5.1	6.4	42.9	0.1	3
LP133−373[b]	14.0400	50.6000	0.20	308	14.0	9.9	19.0	4.7	-9.0	6.5	5.4	5.9	21.7	0.3	1
LP799−74	14.1600	-18.4833	0.19	133	29.8	6.1	-59.6	2.9	-22.8	3.1	-18.6	4.4	66.5	0.1	1
LP66−587	14.2683	63.3000	0.09	140	13.2	18.9	-61.8	9.2	-1.1	13.2	14.3	9.9	63.5	0.2	3
G200−40	14.4330	54.0167	0.39	294	33.7	7.8	78.2	3.9	-29.8	5.2	38.2	4.4	91.9	0.1	3
LP135−155	15.1761	56.6033	0.38	217	13.6	9.8	-54.1	5.3	-98.6	6.6	80.6	5.0	138.3	0.1	2
LP223−14	15.4250	43.3917	0.14	186	32.5	5.1	-246.9	3.1	-163.1	3.1	77.0	2.6	305.7	0.0	3
LP176−59	15.5533	46.9833	0.51	296	11.5	10.6	89.6	6.3	-54.7	6.7	58.0	5.3	120.0	0.1	3

TABLE 5 — *Continued*

Identifier (dM) (1)	R.A. (B1950) (2)	Decl. (B1950) (3)	μ ($''$/yr) (4)	Θ (deg) (5)	v_r (km/s) (6)	σ_{v_r} (km/s) (7)	U (km/s) (8)	σ_U (km/s) (9)	V (km/s) (10)	σ_V (km/s) (11)	W (km/s) (12)	σ_W (km/s) (13)	Sp.V. (km/s) (14)	$\sigma_{\rm Sp.V.}$ (km/s) (15)	Ref. (16)
LP743−25	15.6533	-13.7833	0.20	314	34.6	11.9	12.6	8.4	-11.5	5.8	93.7	6.2	95.2	0.1	3
L480−84	15.7592	-38.1667	0.09	162	79.4	···	-82.2	···	-58.5	···	-25.8	···	104.1	···	3
LP916−26	15.7003	-27.5000	0.24	235	-8.1	6.7	11.9	4.5	-50.9	3.6	-5.9	3.4	52.6	0.1	3
LP42−195	15.8333	71.6833	0.14	4	2.5	9.3	-2.8	4.8	-9.0	6.7	-8.7	4.3	12.8	0.5	2
G152−B4A	15.9228	-08.9917	0.12	198	36.2	17.8	-45.6	13.2	-37.0	8.4	3.3	8.5	58.8	0.2	3
L266−195	16.3833	-54.0833	0.08	12	74.4	···	-81.6	···	-35.4	···	-2.5	···	88.9	···	3
LP101−15	16.5583	57.2500	1.62	319	3.4	12.5	57.0	7.5	-28.3	8.4	21.5	5.4	67.2	0.1	1
LP505−43	16.5833	11.2667	0.17	159	1.3	2.2	-49.1	1.8	-35.2	1.0	-40.3	0.8	72.6	0.0	3
LP686−33	16.9367	-06.1833	0.35	111	-24.8	9.0	-12.1	7.5	6.3	4.1	-92.9	2.7	93.9	0.1	2
LP387−37	17.0650	26.1667	0.28	185	3.9	6.7	-40.6	5.3	-30.9	3.5	-11.1	2.2	52.2	0.1	3
Wolf 672B	17.2681	02.0033	0.50	232	-19.0	1.9	-7.3	1.6	-73.9	0.9	8.4	0.5	74.7	0.0	3
LP101−409	17.2683	59.8500	0.18	355	4.4	21.7	46.5	13.0	-7.1	14.8	-4.5	9.1	47.2	0.3	3
LP101−410	17.2683	59.8500	0.18	355	3.7	18.8	43.0	11.3	-7.8	12.8	-4.9	7.8	44.0	0.3	3
G154−B5A	17.7178	-13.2883	0.09	25	-2.2	3.8	-2.7	3.3	3.8	1.8	-5.6	0.8	7.3	0.4	3
LP44−311	18.4667	69.9667	0.08	355	29.7	9.5	109.5	5.2	-16.9	6.8	25.5	4.2	113.7	0.1	3
LP230−21	18.9917	42.9333	0.26	201	-10.2	11.4	-75.8	8.0	-41.8	6.9	-11.5	4.3	87.3	0.1	2
G142−B2B	19.1889	13.5217	0.10	180	2.7	1.9	-21.0	1.6	-19.1	0.9	-14.1	0.6	31.7	0.0	3
L923−22	19.2983	-07.7500	0.20	198	36.1	13.3	-46.9	10.9	-7.7	6.2	-15.4	4.6	50.0	0.2	3
LP45−216	19.3883	71.5167	0.16	8	33.2	9.8	66.2	5.2	-2.8	7.1	16.7	4.4	68.3	0.1	3
L852−36	19.5483	-13.6000	0.14	189	54.0	4.8	-75.4	3.8	-40.1	2.3	-36.7	1.9	92.9	0.0	3
LP813−18	19.7197	-17.4333	0.24	174	47.5	7.4	-60.0	5.7	-39.9	3.6	-47.4	3.1	86.2	0.1	3
G24−10	20.1922	06.5417	0.70	206	30.0	5.5	-71.7	4.0	-30.1	2.6	-19.4	2.7	80.1	0.1	3
LP575−18	20.4600	06.7500	0.22	32	54.2	25.5	21.1	17.8	78.3	12.0	-24.3	13.8	84.7	0.2	3
LP575−15	20.4600	70.3333	0.26	135	27.9	3.7	-12.3	1.9	37.2	2.7	-61.1	1.7	72.6	0.0	3
LP696−5	20.7450	-04.3000	0.20	199	26.0	5.0	-83.1	3.3	-68.2	2.4	-33.0	2.9	112.5	0.0	3
Ross 193	20.9017	-04.9500	0.82	105	-8.1	11.1	15.9	7.0	-23.1	5.3	-35.4	6.8	45.1	0.2	1
G212−B1B	21.1331	42.7356	0.20	98	2.2	6.9	26.4	3.8	-10.2	4.2	-57.6	3.9	64.2	0.1	3
LP26−184	21.2867	76.5000	0.08	50	12.5	26.0	36.9	12.7	-15.2	19.0	-9.2	12.3	40.9	0.5	3
LP696−5	21.5133	-06.4000	0.33	205	-2.5	3.8	-120.4	2.0	-128.5	1.8	-16.9	2.7	176.9	0.0	3
LP187−6	21.5575	46.3383	0.46	200	3.1	8.5	-92.3	4.3	-9.7	5.4	-51.2	5.0	106.0	0.1	3
LP398−19	21.6417	21.4500	0.12	195	-0.8	7.0	-88.9	3.5	-54.8	3.7	-52.9	4.8	117.0	0.0	3
LP699−29	22.0300	-03.7667	0.24	90	1.5	9.1	83.9	4.0	-28.7	4.4	-77.9	6.9	118.0	0.1	3
LP343−35	22.2167	31.7167	0.13	188	5.3	8.2	-31.5	3.5	-15.6	4.7	-30.4	5.8	46.4	0.1	3
LP188−1	22.4031	48.3617	0.59	41	-10.8	8.0	18.2	3.5	-26.3	5.2	3.3	5.1	32.1	0.2	3
LP400−21	22.5683	22.2800	0.20	74	7.4	9.1	75.0	3.2	-14.9	4.8	-35.5	7.0	84.3	0.1	3
LP761−113	22.8222	-10.5333	0.19	157	20.5	1.7	-17.9	0.5	-40.7	0.9	-44.1	1.4	62.6	0.0	3
LP2−696	22.8867	81.2333	0.23	63	34.1	10.0	44.8	4.8	-4.6	7.4	4.4	4.7	45.3	0.2	3
LP581−36	22.8900	05.5000	0.45	127	51.6	1.6	0.0	0.4	-4.6	0.8	-72.6	1.3	72.7	0.0	3
LP345−26	22.9383	31.3167	0.15	70	26.5	6.1	34.8	2.0	4.7	3.5	-23.4	4.6	42.2	0.1	2
LP401−49	23.0967	23.9667	0.24	108	-7.2	13.3	51.4	3.7	-58.5	7.2	-57.6	10.6	96.8	0.1	3
LP933−66	23.1594	-27.6267	0.21	98	3.6	7.2	42.8	2.1	-41.5	4.0	-35.0	5.6	69.1	0.1	3
LP522−35	23.3000	12.7000	0.18	72	11.6	8.9	42.9	1.8	-11.6	4.5	-22.1	7.5	49.7	0.1	3
LP762−53	23.3089	-13.7333	0.20	150	-1.2	10.2	-6.1	2.1	-63.5	5.2	-27.5	8.5	69.5	0.1	1
LP582−42	23.3250	09.5000	0.19	225	9.9	8.5	-82.2	1.6	-20.6	4.3	-27.8	7.2	89.2	0.1	3
G275−B16B	23.3917	-24.1817	0.06	175	33.9	21.1	-51.9	5.1	-100.4	11.5	-50.1	17.0	123.6	0.1	3
LP77−37A	23.5717	64.6217	0.21	114	19.3	8.4	50.6	3.7	-15.7	5.9	-53.4	4.7	75.2	0.1	2
LP463−27	23.6067	20.7500	0.33	58	32.5	7.3	37.7	1.5	10.0	3.9	-20.9	6.0	44.3	0.1	1
LP191−9	23.6892	47.1500	0.31	94	14.7	4.2	79.8	1.5	-39.6	2.7	-42.3	2.9	98.6	0.0	2
LP347−5	23.6900	32.2700	0.24	256	15.7	3.4	-12.5	0.9	3.7	2.0	-14.1	2.6	19.2	0.1	3
G273−B15A	23.6958	-16.4583	0.14	210	25.5	2.3	-55.2	0.4	-32.1	1.2	-33.4	1.9	72.0	0.0	3
LP935−14	23.7433	-26.6650	0.36	255	49.6	5.7	-91.1	1.3	7.2	3.2	-37.8	4.6	98.9	0.0	3
LP577−72	23.8586	-33.5467	0.50	217	40.8	···	-61.7	···	-34.4	···	-36.4	···	79.4	···	3
LP524−35	23.9033	05.3833	0.21	69	31.7	8.3	55.0	0.7	-3.8	4.1	-33.1	7.2	64.3	0.1	3
LP348−20	23.9817	27.0500	0.11	106	17.9	8.9	40.1	2.0	-31.5	4.9	-41.8	7.1	65.9	0.1	3

TABLE 5 — *Continued*

Identifier (dM) (1)	R.A. (B1950) (2)	Decl. (B1950) (3)	μ ($''$/yr) (4)	Θ (deg) (5)	v_r (km/s) (6)	σ_{v_r} (km/s) (7)	U (km/s) (8)	σ_U (km/s) (9)	V (km/s) (10)	σ_V (km/s) (11)	W (km/s) (12)	σ_W (km/s) (13)	Sp (k (

REFERENCES. — (1) dMe Stars; (2) dM(e) Stars; (3) dM Stars; (4) V and M_V are from the WD companion.

NOTE. — Units of right ascension are hours, and units of declination are degrees.

[a] Stellar halo white dwarf candidate.

[b] M dwarf has close (eclipsing) companion.